JCAMECH

Vol. 51, No. 2, December 2020, pp 340-360

DOI: 10.22059/jcamech.2020.296400.474

Size-dependent thermoelastic analysis of rotating nanodisks of variable thickness

*Abbas Barati[a], Mehdi mousavi Khoram[b], Mohammad Shishesaz[b], Mohammad Hosseini[b,c *]*

[a] *Department of Mechanical Engineering, University of Guilan, Rasht, Iran*
[b] *Department of Mechanical Engineering, Shahid Chamran University of Ahvaz, Ahvaz, Iran*
[c] *Department of Mechanical Engineering, University of Hormozgan, Bandar-Abbas, Iran*

ARTICLE INFO

Article history:
Received: 22 January 2020
Accepted: 30 February 2020

Keywords:
Nanodisk,
Strain gradient theory,
Thermoelastic analysis,
Angular velocity.

ABSTRACT

This paper contains a strain gradient theory to capture size effects in rotating nanodisks of variable thickness under thermal and mechanical loading. Material properties of nanodisks have been taken homogeneous material. The strain gradient theory and the Hamilton's principle are employed to derive the governing equations. Due to complexity of the governing differential equation and boundary conditions, numerical schemes are used to solve the problem. In the following, some numerical results are presented to show the influence of size effect on stress analysis of rotating nanodisks. Results show that the stresses of rotating nanodisks is strongly sensitive to the length scale material parameters.

1. Introduction

Nanotechnology has a great contribution in the development of engineering and medicine fields. One of the most useful nanostructures are nanodiscs [1]. Circular nanodisk is a common component of nanoelectromechanical systems (NEMS) [2] that exposed to mechanical and thermal loading. The classical elasticity theory is used for a continuum structures, but in nano-scale, classical continuum approaches do not adequately address the atomistic nature of the nano-size structures [3-25]. experimental studies show that size effect is important in nano-scale [26]. Since the experimental studies of nanostructures are difficult, the molecular dynamics (MD) simulations have become the eminent tool in order to model and study the nanostructures and their mechanical behaviors; but it is computationally expensive for structures with a large number of atoms [18-20, 27]. In last decades, some non-classical continuum mechanics theories are introduced to capture size effect [28-35]. Among the non-classical continuum mechanics theories, strain gradient theory [36] has been widely used to analyze the nanostructures. According to this theory, the strain energy of the nanostructure is dependent on gradients of strain in addition to strains [37].

In recent years, much research has been done in the field of nanotechnology [38-40]. Rahimi *et al.* [41] studied thermo-mechanical free vibration and buckling of a curved functionally graded microbeam in the framework of strain gradient theory. The Timoshenko beam model was used to examine the behavior of microstructures. The material properties of microbeam vary according to power-law exponent in the thickness direction. Also, Hamilton's principle was used in order to obtain the equilibrium equation and boundary conditions. In their study the effects of some parameters such as length scale parameter, variation of material properties and temperature were investigated. Results indicate that natural frequency of functionally graded microbeams under thermo-mechanical loading are more sensitive to geometrical, physical and mechanical properties. A flexoelectric theory was offered by Li *et al.* [42] in order to study the size dependent electromechanical coupling behaviors of circular micro-plate. In this research, static bending and free vibration behaviors of simply supported circular microplate were studied. Findings indicate that bending behaviors and natural frequency of this microplate are dependent on the size effects. Free vibration of through the thickness functionally graded nanobeams on the viscoelastic foundation was investigated by Ebrahimi and Barati [43]. Surface stress effects were considered for viscoelastic

*Corresponding author. *Tel:* +989163006273

E-mail addresses: s.m.hssini@gmail.com, m-hosseini@phdstu.scu.ac.ir (M. Hosseini).

foundation and material properties vary according to power-law model. Also, Euler-Bernoulli beam model was utilized in order to analyze the behavior of nanobeams. Results of this study demonstrate that the frequency of a functionally graded nanobeam decreases when the nonlocal parameters were taken into account. Considering the length scale parameters increase the frequency and stiffness of FG nanobeam. Moreover, damping coefficient will reduce the vibration frequency. In another study, Ebrahimi and Barati [44] investigated the wave propagation of size-dependent functionally graded nanobeams. They analyze this problem by using of nonlocal strain gradient theory and consider the thermal effects. Governing equations were derived by using of Hamilton's principle. Results show that phase velocity and wave frequency have reverse proportion to temperature rise. Zhang *et al.* [45] suggested a size-dependent model for the nonlinear static behavior of damaged piezoelectric cantilever microbeams in the framework of modified couple stress theory. They use Hamilton's principle in order to formulate the problem. Their study illustrates that the size effect has a significant influence on the nonlinear static behavior of these microstructures. Tavakolian and Farrokhabadi [46] developed a novel model for the dynamic instability of Euler-Bernoulli nanobeams in the thermal environment by using of nonlocal elasticity theory. Nonlinear dynamic governing equation was solved numerically. The effects of some parameters such as nonlocal parameter and temperature on the dynamic pull-in instability of double clamped nanobeams were studied. Raahemifar [47] investigated symmetric and asymmetric size-dependent buckling of initially curved shallow Euler-Bernoulli nanobeams based on the strain gradient theory. Results indicate that the size effects play an important role in the buckling and pull-in instability of a nanobeam. Size-dependent free transverse vibration of through-thickness functionally graded Timoshenko cracked nanobeams was studied by Soltanpour et al. [48] by using of nonlocal elasticity theory. It was assumed that the nanobeam was resting on the Winkler elastic foundation and material properties vary according to power-law distribution. Hamilton's principle was employed in order to derive the equation of motion and associated boundary condition of FG nanobeams. Findings indicate that nonlocal parameters, mode number and crack position have significant effects on the free vibration behavior of FG cracked nanobeams. Ghayesh *et al.* [49] developed a numerical method in order to simulate the complex motion of three−layered Timoshenko microarches. Modified couple stress theory was used to consider the size effects. Soleimani *et al.* [50] offered an isogeometric finite element method for buckling behavior of graphene sheets based on the nonlocal elasticity and first-order shear deformation plate theories. Results show that buckling loads are affected by size effects. Based on the modified couple stress theory, a nonlinear third-order shear-deformable model for dynamic analysis of microplates which resting on the elastic foundation was presented by Ghayesh *et al*. [51]. It is observed that the natural frequency is directly proportional to linear stiffness coefficient of elastic foundation and has a reverse proportion to the thickness ratio. Golmakani and Vahabi [52] examined axisymmetric buckling behaviors of functionally graded annular nanoplates which embedded in a Pasternak elastic foundation on the basis of nonlocal elasticity and first order shear deformation theories. Variation of material properties were according to the power-law distribution. This study indicates that buckling loads are independent of boundary conditions. Moreover, buckling loads have a positive relation to thickness-to-radius ratio. Peng *et al.* [53] offered a new analytical model for the nonlinear behavior of electrostatically actuated micro-actuators based on the symmetric stress gradient elasticity theory. It was observed that symmetric stress gradient elasticity theory predict stiffer micro-beam compared with classical elasticity theory. Size effect have a significant effect on the nonlinear dynamic behavior of micro-actuators for smaller values of initial gap, length and height of beam along with higher values of voltage. Ansari *et al.* [54] investigated the linear and nonlinear vibration behavior of viscoelastic micro/nano-beams in the framework of modified strain gradient theory. Timoshenko beam model was considered. Findings show that fractional order and thickness-to-length scale parameter have revers effects on the frequency of size-dependent viscoelastic beams. Gholami and Ansari [55] studied free vibration behavior of functionally graded rectangular microplates on the basis of strain gradient theory. Based on the strain gradient elasticity and Kirchhoff plate theories, free vibration and pull-in instability of circular microplates were investigated by Mohammadi *et al.* [56]. They were considered hydrostatic and electrostatic forces simultaneously. Hosseini *et al.* [17] analyzed mechanical behaviors of functionally graded rotating nanodisks of nonlinear variable thickness. Their research indicate that equilibrium equation and boundary conditions of nanodisk are different from those of macro-scale disk. Ramezani [57] suggested a model in the framework of first-strain gradient elasticity theory in order to investigate nonlinear free vibration behavior of Kirchhoff microplate. Ansari *et al*. [58] studied the nonlinear vibration behavior of multiwalled carbon nanotubes subjected to temperature effect based on the nonlocal elasticity theory. Also, many other researches have done in the field of non-classical elasticity theory [59-63].

Previous literature review shows that little attention has been to the mechanical and thermal behaviors of rotating nanodisks of variable thickness. Therefore, in this paper, fundamental equations of nanodisks are presented based on the non-classical continuum mechanics. The equilibrium equation and boundary conditions of nanodisks are obtained in the sec. 2. Then, numerical results and diagrams have been provided in the sec. 3. Finally, the results are summarized in sec. 4.

2. Theory and formulation

Fig. 1 shows the geometry of a nanodisk. The thickness of nanodisk is a function of radius (r). Temperature at inner radius, temperature at outer radius, internal and external pressure (pressure at inner and outer radii) are T_i, T_o, $\hat{\sigma}_i$ and $\hat{\sigma}_o$, respectively. The nanodisk rotates with constant angular velocity, ω. It is assumed that the disk thickness is too small compared to its radii. Furthermore, assuming plane stress condition, the radial loads are allowed to vary along the disk radius while the tangential components of the load are taken to be zero.

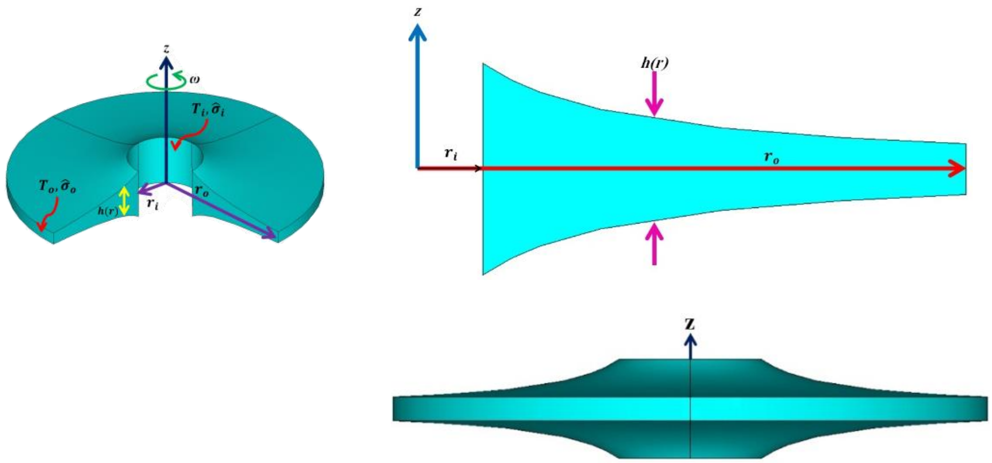

Fig. 1. A rotating nanodisk of variable thickness

In order to derive the governing equations, strain gradient theory is applied. It is assumed that rotating nanodisk of variable thickness is subjected to a radial varying temperature field. In classical elasticity theory, strain energy density function is dependent on the infinitesimal strain tensor (which is the symmetric portion of the gradient of radial displacement field u). One can point out that the strain tensor ε and gradient of strain tensor ξ can be written as:

$$\boldsymbol{\varepsilon}=\frac{1}{2}\left[\nabla u+(\nabla u)^{T}\right] \tag{1}$$

$$\boldsymbol{\xi}=\nabla\boldsymbol{\varepsilon}=\frac{1}{2}\nabla\left[\nabla u+(\nabla u)^{T}\right]$$

where

$$\nabla=e_r\frac{\partial}{\partial r}+e_\theta\frac{1}{r}\frac{\partial}{\partial\theta}+e_z\frac{\partial}{\partial z} \tag{2}$$

The components of the strain tensor with thermal strains may be written as [64];

$$\varepsilon_r=\frac{\partial u}{\partial r}+\alpha\Delta T,\ \varepsilon_\theta=\frac{u}{r}+\alpha\Delta T,\ \varepsilon_{ij}=0\ if\ i\neq j \tag{3}$$

In Eq. (3), α and T are the coefficient of thermal expansion coefficient and temperature at any radius, respectively. One can show that the components of gradient of strains, in presence of a temperature field are:

$$\xi_{rrr}=\frac{\partial\left(\dfrac{\partial u}{\partial r}+\alpha\Delta T\right)}{\partial r},\ \xi_{r\theta\theta}=\frac{\partial\left(\dfrac{u}{r}+\alpha\Delta T\right)}{\partial r},$$
$$\xi_{\theta\theta r}=\frac{\partial\left(\dfrac{u}{r}\right)}{\partial r},\qquad \xi_{\theta r\theta}=\frac{\partial\left(\dfrac{u}{r}\right)}{\partial r}. \tag{4}$$

For plane stress conditions, the relationship between stresses and strains is determined using Hooke's Law [65-67];

$$\begin{cases}\sigma_r=\dfrac{E}{(1-\upsilon^2)}\left(\dfrac{du}{dr}+\upsilon\dfrac{u}{r}-(1+\upsilon)\alpha\Delta T\right)\\[2ex] \sigma_\theta=\dfrac{E}{(1-\upsilon^2)}\left(\dfrac{u}{r}+\upsilon\dfrac{du}{dr}-(1+\upsilon)\alpha\Delta T\right)\end{cases} \tag{5}$$

where;

$$A=\frac{E}{\left(1-\upsilon^2\right)},B=\frac{E\upsilon}{\left(1-\upsilon^2\right)},C=\frac{E}{\left(1-\upsilon\right)} \tag{6}$$

where E and υ are the modulus of elasticity and Poisson's ratio, respectively.

High-order stress tensor τ_{ijk} is defined as follows:

$$\begin{aligned}\tau_{ijk}=&\frac{1}{2}a_1\left(\delta_{ij}\xi_{kpp}+2\delta_{jk}\xi_{ppi}+\delta_{ik}\xi_{jpp}\right)\\&+2a_2\delta_{jk}\xi_{ipp}+a_3\left(\delta_{ij}\xi_{ppk}+\delta_{ik}\xi_{ppj}\right)\\&+2a_4\xi_{ijk}+a_5\left(\xi_{jki}+\xi_{kji}\right).\end{aligned} \tag{7}$$

where a_i's and δ_{ij} are the length scale material parameters and Kronecker's delta, respectively. Consequently, expanding Eq. (7) and using Eq. (4) we have:

$$\begin{Bmatrix}\tau_{rrr}\\ \tau_{\theta\theta r}\\ \tau_{r\theta\theta}\end{Bmatrix}=\begin{bmatrix}k_1 & \dfrac{k_2}{r} & -\dfrac{k_2}{r^2}\\ k_3 & \dfrac{k_4}{r} & -\dfrac{k_4}{r^2}\\ k_5 & \dfrac{k_6}{r} & -\dfrac{k_6}{r^2}\end{bmatrix}\begin{Bmatrix}\dfrac{\partial^2 u}{\partial r^2}\\ \dfrac{\partial u}{\partial r}\\ u\end{Bmatrix}+\begin{Bmatrix}D_1\\ D_2\\ D_3\end{Bmatrix}\frac{\partial(\alpha\Delta T)}{\partial r} \tag{8}$$

where

$$\begin{aligned}&k_1=2\left(a_1+a_2+a_3+a_4+a_5\right),\\&k_2=2\left(a_1+a_2+a_3\right),\\&k_3=k_7=1/2\,a_1+a_3,\\&k_4=k_8=1/2\,a_1+a_3+2a_4+2a_5,\\&k_5=\left(a_1+2a_2\right),\\&k_6=\left(a_1+2a_2+2a_4+2a_5\right),\\&D_1=\left(3a_1+4a_2+2a_3+2a_4+2a_5\right),\\&D_2=D_4=\left(a_1+a_3+a_5\right).\\&D_3=\left(a_1+4a_2+2a_4\right)\end{aligned} \tag{9}$$

Now, Hamilton's principle, as given in Eq. (10), is used to derive the governing differential equation and its associated boundary conditions.

$$\int_{t_1}^{t_2}(\delta U-\delta K-\delta W)dt=0 \tag{10}$$

In this equation, *W*, *K* and *U* are the work done by the external loads, kinetic energy and total strain energy, respectively. The variation in total strain energy may be written as;

$$\begin{aligned}\delta U&=\int_V\left(\sigma_{jk}\delta\varepsilon_{jk}+\tau_{ijk}\delta\xi_{ijk}\right)dV\\&=2\pi\int_{r_i}^{r_o}\begin{pmatrix}\sigma_r\delta\varepsilon_r+\sigma_\theta\delta\varepsilon_\theta+\tau_{rrr}\delta\xi_{rrr}\\+\tau_{\theta\theta r}\delta\xi_{\theta\theta r}+\tau_{r\theta\theta}\delta\xi_{r\theta\theta}+\tau_{\theta r\theta}\delta\xi_{\theta r\theta}\end{pmatrix}rhdr\end{aligned} \tag{11}$$

where *h* and *V* are the thickness and volume of the nano-disk, respectively. Note that the temperature distribution is assumed to be only a function of *r*, and hence, along with other assumptions, axisymmetric loading is imposed on the model. Additionally, the expression for variation in work done by external loads is:

$$\delta W=2\pi rh\begin{pmatrix}\hat\sigma_r\delta u+\hat\sigma_\theta\delta v+\hat\tau_{rrr}\delta\varepsilon_{rr}\\+\hat\tau_{r\theta r}\delta\varepsilon_{r\theta}+\hat\tau_{\theta rr}\delta\varepsilon_{\theta r}+\hat\tau_{\theta\theta r}\delta\varepsilon_{\theta\theta}\end{pmatrix} \tag{12}$$

In Eq. (12), the symbols with a hat (^) correspond to the components associated with the external load. Due to axisymmetric loading, the tangential component of the displacement, namely *v*, is zero. Consequently, since additional $\varepsilon_{r\theta}$ and $\varepsilon_{\theta r}$ will be zero, then, Eq. (12) may be simplified as:

$$\delta W=2\pi rh\left(\hat\sigma_r\delta u+\hat\tau_{rrr}\frac{d\delta u}{dr}+\hat\tau_{\theta\theta r}\frac{\delta u}{r}\right) \tag{13}$$

Kinetic energy of the rotating nano-disks can be written as [17];

$$\delta K=2\pi\int_{r_i}^{r_o}\rho r^2h\omega^2\delta u dr \tag{14}$$

where ρ, ω and *h* are the density, angular velocity and nanodisk thickness, respectively. Substituting Eqs.(11), (13) and (14) in Eq. (10), one may conclude that;

$$\int_{r_i}^{r_o}\begin{pmatrix}rh\tau_{rrr}\dfrac{\partial^2\delta u}{\partial r^2}+\left(h\left(r\sigma_r+\tau_{\theta\theta r}+\tau_{r\theta\theta}+\tau_{\theta r\theta}\right)\right)\dfrac{d\delta u}{dr}\\+\left(h\left(\sigma_\theta-\dfrac{\left(\tau_{\theta\theta r}+\tau_{r\theta\theta}+\tau_{\theta r\theta}\right)}{r}-\rho r^2\omega^2\right)\right)\delta u\end{pmatrix}dr-rh\left(\left(\hat\sigma_r+\frac{\hat\tau_{\theta\theta r}}{r}\right)\delta u+\hat\tau_{rrr}\frac{d\delta u}{dr}\right)=0 \tag{15}$$

Using integration by parts along with variational principle, Eq. (15) may be simplified as;

$$\begin{aligned}&\int_{r_i}^{r_o}\left(\frac{d^2\left(rh\tau_{rrr}\right)}{dr^2}-\frac{d\left(h\left(r\sigma_r+\tau_{\theta\theta r}+\tau_{r\theta\theta}+\tau_{\theta r\theta}\right)\right)}{dr}+h\left(\sigma_\theta-\frac{\left(\tau_{\theta\theta r}+\tau_{r\theta\theta}+\tau_{\theta r\theta}\right)}{r}-\rho r^2\omega^2\right)\right)\delta u dr\\&+\left(rh\tau_{rrr}-rh\hat\tau_{rrr}\right)\frac{\partial\delta u}{\partial r}\bigg|_{r_i}^{r_o}+\left(h\left(r\sigma_r+\tau_{\theta\theta r}+\tau_{r\theta\theta}+\tau_{\theta r\theta}\right)-\frac{d\left(rh\tau_{rrr}\right)}{dr}-rh\left(\hat\sigma_r+\frac{\hat\tau_{\theta\theta r}}{r}\right)\right)\delta u\bigg|_{r_i}^{r_o}=0\end{aligned} \tag{16}$$

One may use Eq. (16) to deduce the equilibrium equation and its associated boundary conditions in terms of Eq. (17).

$$\begin{aligned}&\textit{equilibrium Equation}:\\&\frac{d^2\left(rh\tau_{rrr}\right)}{dr^2}-\frac{d\left(h\left(r\sigma_r+\tau_{\theta\theta r}+\tau_{r\theta\theta}+\tau_{\theta r\theta}\right)\right)}{dr}+h\left(\sigma_\theta-\frac{\left(\tau_{\theta\theta r}+\tau_{r\theta\theta}+\tau_{\theta r\theta}\right)}{r}-\rho r^2\omega^2\right)=0\\&\textit{Boundary Conditions}:\\&rh\tau_{rrr}-rh\hat\tau_{rrr}=0\quad or\quad \tau_{rrr}=\hat\tau_{rrr}\quad @r=r_1,r_2\\&h\left(r\sigma_r+\tau_{\theta\theta r}+\tau_{r\theta\theta}+\tau_{\theta r\theta}\right)-\frac{d\left(rh\tau_{rrr}\right)}{dr}-rh\left(\hat\sigma_r+\frac{\hat\tau_{\theta\theta r}}{r}\right)=0\quad @r=r_1,r_2\end{aligned} \tag{17}$$

Substituting Eqs. (5), (6) and (8) in Eqs. (17), one may write the differential equilibrium equation.

$$
\begin{aligned}
& rhk_1\frac{d^4u}{dr^4}+\left(2r\left(\frac{dh}{dr}k_1\right)+h\left(2k_1+k_2-k_3-k_5-k_7\right)\right)\frac{d^3u}{dr^3}+\begin{pmatrix} -Ahr+r\left(\dfrac{d^2h}{dr^2}k_1\right)+\dfrac{dh}{dr}\left(2k_1+2k_2-k_3-k_5-k_7\right) \\ -\dfrac{1}{r}h\left(k_2+k_3+k_4+k_5+k_6+k_7+k_8\right) \end{pmatrix}\frac{d^2u}{dr^2} \\
& +\begin{pmatrix} -\left(Ar\dfrac{dh}{dr}+Ah\right)+\left(\dfrac{d^2h}{dr^2}k_2\right)-\dfrac{1}{r}\dfrac{dh}{dr}\left(2k_2+k_4+k_6+k_8\right) \\ +\dfrac{1}{r^2}h\left(2k_2+k_4+k_6+k_8\right) \end{pmatrix}\frac{du}{dr}+\begin{pmatrix} -B\dfrac{dh}{dr}+\dfrac{1}{r}Ah-\dfrac{1}{r}\left(\dfrac{d^2h}{dr^2}k_2\right)+\dfrac{1}{r^2}\dfrac{dh}{dr}\left(2k_2+k_4+k_6+k_8\right) \\ -\dfrac{1}{r^3}h\left(2k_2+k_4+k_6+k_8\right) \end{pmatrix}u \\
& +r\left(\frac{dh}{dr}C\right)\left(\alpha\Delta T\right)+\begin{pmatrix} r\dfrac{d^2h}{dr^2}D_1+\dfrac{dh}{dr}\left(2D_1-D_2-D_3-D_4\right) \\ +hCr-\dfrac{1}{r}h\left(D_2+D_3+D_4\right) \end{pmatrix}\frac{d\left(\alpha\Delta T\right)}{dr} \\
& +\left(2r\frac{dh}{dr}D_1+h\left(2D_1-D_2-D_3-D_4\right)\right)\frac{d^2\left(\alpha\Delta T\right)}{dr^2}+rhD_1\frac{d^3\left(\alpha\Delta T\right)}{dr^3}=\rho r^2\omega^2 h
\end{aligned}
\tag{18}
$$

Similarly, for the boundary conditions we have;

(B. C. 1)

$$
k_1\frac{d^2u}{dr^2}+\frac{1}{r}k_2\frac{du}{dr}-\frac{1}{r^2}k_2u+D_1\frac{d\left(\alpha\Delta T\right)}{dr}=\hat{\tau}_{rrr} \qquad @r=r_i,r_o \tag{19}
$$

and (B. C. 2)

$$
\begin{aligned}
& -rhk_1\frac{d^3u}{dr^3}-\left(r\left(\frac{dh}{dr}k_1\right)+h\left(k_1+k_2-k_3-k_5-k_7\right)\right)\frac{d^2u}{dr^2}+\left(Ahr+\frac{1}{r}h\left(k_2+k_4+k_6+k_8\right)-\left(\frac{dh}{dr}k_2\right)\right)\frac{du}{dr} \\
& +\left(Bh-\frac{1}{r^2}h\left(k_2+k_4+k_6+k_8\right)+\frac{1}{r}\left(\frac{dh}{dr}k_2\right)\right)u-hCr\left(\alpha\Delta T\right)-\left(r\frac{dh}{dr}D_1+h\left(D_1-D_2-D_3-D_4\right)\right)\frac{d\left(\alpha\Delta T\right)}{dr} \\
& -rhD_1\frac{d^2\left(\alpha\Delta T\right)}{dr^2}=rh\left(\hat{\sigma}_r+\frac{\hat{\tau}_{\theta\theta r}}{r}\right) \qquad @r=r_i,r_o
\end{aligned}
\tag{20}
$$

Finally, the total stresses are calculated as follows.

$$
\begin{aligned}
\sigma_r^t &= \sigma_r-\frac{d\left(\tau_{rrr}\right)}{dr}+\frac{\tau_{r\theta\theta}+\tau_{\theta r\theta}-\tau_{rrr}}{r} \\
\sigma_\theta^t &= \sigma_\theta-\frac{d\left(\tau_{\theta\theta r}\right)}{dr}+\frac{\tau_{r\theta\theta}+\tau_{\theta r\theta}-\tau_{\theta\theta r}}{r}
\end{aligned}
\tag{21}
$$

Now, for simplicity and an easier solution, these equations are non-dimensionalized. For this purpose, the following non-dimensional parameters are defined.

$$
\begin{aligned}
& \bar{r}=\frac{r}{r_o}, \qquad \bar{A}=\frac{A}{E}, \quad \bar{C}=\frac{C}{E}, \qquad \bar{\alpha}=\frac{\alpha}{\alpha}, \qquad \bar{k}_j=\frac{k_j}{Er_o^2} \quad j=1,2,\ldots,8 \\
& \bar{u}\left(\bar{r}\right)=\frac{u\left(r\right)}{u_o}, \quad \bar{B}=\frac{B}{E}, \quad \bar{\gamma}=\frac{\rho_o\omega^2r_o^2}{E}, \quad \Delta\bar{T}\left(\bar{r}\right)=\frac{\Delta T\left(r\right)}{\Delta T_o}, \quad \bar{D}_j=\frac{D_j}{Er_o^2} \quad j=1,2,3,4 \\
& \bar{\sigma}_r=\frac{\sigma_r}{E}, \quad \bar{\sigma}_\theta=\frac{\sigma_\theta}{E}, \quad \bar{\tau}_{ijk}=\frac{\tau_{ijk}}{Er_o} \\
& \bar{\hat{\sigma}}_r=\frac{\hat{\sigma}_r}{E}, \quad \bar{\hat{\sigma}}_\theta=\frac{\hat{\sigma}_\theta}{E}, \quad \bar{\hat{\tau}}_{ijk}=\frac{\hat{\tau}_{ijk}}{Er_o}
\end{aligned}
\tag{22}
$$

where;

$$
\begin{aligned}
u_o &= \frac{\rho\omega^2r_o^3}{E}+r_o\alpha\Delta T_o \\
\Delta T_o &= T_o-T_i \\
\Delta T\left(r\right) &= T\left(r\right)-T_i
\end{aligned}
$$

Therefore, Eqs. (18)–(20) can be written in a non-dimensional form as;

$$
\begin{aligned}
&\bar{r}\bar{h}\bar{k}_1\frac{d^4\bar{u}(\bar{r})}{d\bar{r}^4}+\left(2\bar{r}\left(\frac{d\bar{h}}{d\bar{r}}\bar{k}_1\right)+\bar{h}\left(2\bar{k}_1+\bar{k}_2-\bar{k}_3-\bar{k}_5-\bar{k}_7\right)\right)\frac{d^3\bar{u}}{d\bar{r}^3}\\
&+\begin{pmatrix}-\bar{A}\bar{h}\bar{r}+\bar{r}\left(\frac{d^2\bar{h}}{d\bar{r}^2}\bar{k}_1\right)+\frac{d\bar{h}}{d\bar{r}}\left(2\bar{k}_1+2\bar{k}_2-\bar{k}_3-\bar{k}_5-\bar{k}_7\right)\\-\frac{1}{\bar{r}}\bar{h}\left(\bar{k}_2+\bar{k}_3+\bar{k}_4+\bar{k}_5+\bar{k}_6+\bar{k}_7+\bar{k}_8\right)\end{pmatrix}\frac{d^2\bar{u}}{d\bar{r}^2}\\
&+\begin{pmatrix}-\left(\bar{A}\bar{r}\frac{d\bar{h}}{d\bar{r}}+\bar{A}\bar{h}\right)+\left(\frac{d^2\bar{h}}{d\bar{r}^2}\bar{k}_2\right)-\frac{1}{\bar{r}}\frac{d\bar{h}}{d\bar{r}}\left(2\bar{k}_2+\bar{k}_4+\bar{k}_6+\bar{k}_8\right)\\+\frac{1}{\bar{r}^2}\bar{h}\left(2\bar{k}_2+\bar{k}_4+\bar{k}_6+\bar{k}_8\right)\end{pmatrix}\frac{d\bar{u}}{d\bar{r}}\\
&+\begin{pmatrix}-\left(\bar{B}\frac{d\bar{h}}{d\bar{r}}\right)+\frac{1}{\bar{r}}\bar{A}\bar{h}-\frac{1}{\bar{r}}\left(\frac{d^2\bar{h}}{d\bar{r}^2}\bar{k}_2\right)\\+\frac{1}{\bar{r}^2}\frac{d\bar{h}}{d\bar{r}}\left(2\bar{k}_2+\bar{k}_4+\bar{k}_6+\bar{k}_8\right)-\frac{1}{\bar{r}^3}\bar{h}\left(2\bar{k}_2+\bar{k}_4+\bar{k}_6+\bar{k}_8\right)\end{pmatrix}\bar{u}\\
&+\frac{r_o}{u_o}\alpha\Delta T_o\bar{r}\left(\frac{d\bar{h}}{d\bar{r}}\bar{C}\right)\left(\bar{\alpha}\Delta\bar{T}\right)+\frac{r_o}{u_o}\alpha\Delta T_o\begin{pmatrix}\bar{r}\frac{d^2\bar{h}}{d\bar{r}^2}\bar{D}_1+\frac{d\bar{h}}{d\bar{r}}\left(2\bar{D}_1-\bar{D}_2-\bar{D}_3-\bar{D}_4\right)\\+\bar{h}\bar{C}\bar{r}-\frac{1}{\bar{r}}\bar{h}\left(\bar{D}_2+\bar{D}_3+\bar{D}_4\right)\end{pmatrix}\frac{d\left(\bar{\alpha}\Delta\bar{T}\right)}{d\bar{r}}\\
&+\frac{r_o}{u_o}\alpha\Delta T_o\left(2\bar{r}\frac{d\bar{h}}{d\bar{r}}\bar{D}_1+\bar{h}\left(2\bar{D}_1-\bar{D}_2-\bar{D}_3-\bar{D}_4\right)\right)\frac{d^2\left(\bar{\alpha}\Delta\bar{T}\right)}{d\bar{r}^2}+\frac{r_o}{u_o}\alpha\Delta T_o\bar{r}\bar{h}\bar{D}_1\frac{d^3\left(\bar{\alpha}\Delta\bar{T}\right)}{d\bar{r}^3}=\frac{r_o}{u_o}\bar{\gamma}\bar{\rho}\bar{r}^2\bar{h}
\end{aligned}
\tag{23}
$$

B. C. 1;

$$
\left(\bar{k}_1\frac{d^2\bar{u}}{d\bar{r}^2}+\frac{1}{\bar{r}}\bar{k}_2\frac{d\bar{u}}{d\bar{r}}-\frac{1}{\bar{r}^2}\bar{k}_2\bar{u}\right)+\frac{r_o}{u_o}\alpha\Delta T_o\bar{D}_1\frac{d\left(\bar{\alpha}\Delta\bar{T}\right)}{d\bar{r}}=\frac{r_o}{u_o}\bar{\hat{\tau}}_{rrr}\quad @\bar{r}=\bar{r}_i,1
\tag{24}
$$

and B. C. 2;

$$
\begin{aligned}
&-\bar{r}\bar{h}\bar{k}_1\frac{d^3\bar{u}}{d\bar{r}^3}-\left(\bar{r}\left(\frac{d\bar{h}}{d\bar{r}}\bar{k}_1\right)+\bar{h}\left(\bar{k}_1+\bar{k}_2-\bar{k}_3-\bar{k}_5-\bar{k}_7\right)\right)\frac{d^2\bar{u}}{d\bar{r}^2}\\
&+\left(\bar{A}\bar{h}\bar{r}+\frac{1}{\bar{r}}\bar{h}\left(\bar{k}_2+\bar{k}_4+\bar{k}_6+\bar{k}_8\right)-\left(\frac{d\bar{h}}{d\bar{r}}\bar{k}_2\right)\right)\frac{d\bar{u}}{d\bar{r}}\\
&+\left(\bar{B}\bar{h}-\frac{1}{\bar{r}^2}\bar{h}\left(\bar{k}_2+\bar{k}_4+\bar{k}_6+\bar{k}_8\right)+\frac{1}{\bar{r}}\left(\frac{d\bar{h}}{d\bar{r}}\bar{k}_2\right)\right)\bar{u}\\
&-\frac{r_o}{u_o}\alpha\Delta T_o\bar{h}\bar{C}\bar{r}\left(\bar{\alpha}\Delta\bar{T}\right)-\frac{r_o}{u_o}\alpha\Delta T_o\left(\bar{r}\frac{d\bar{h}}{d\bar{r}}\bar{D}_1+\bar{h}\left(\bar{D}_1-\bar{D}_2-\bar{D}_3-\bar{D}_4\right)\right)\frac{d\left(\bar{\alpha}\Delta\bar{T}\right)}{d\bar{r}}\\
&-\frac{r_o}{u_o}\alpha\Delta T_o\bar{r}\bar{h}\bar{D}_1\frac{d^2\left(\bar{\alpha}\Delta\bar{T}\right)}{d\bar{r}^2}=\frac{r_o}{u_o}\bar{r}\bar{h}\left(\bar{\hat{\sigma}}_r+\frac{\bar{\hat{\tau}}_{\theta\theta r}}{\bar{r}}\right)\qquad @\bar{r}=\bar{r}_i,1
\end{aligned}
\tag{25}
$$

If the size effect coefficients are taken to zero ($a_1=a_2=a_3=a_4=a_5=0$), then the above equations reduce to those of classic solution. In this case, Eq. (24) is vanished and the equilibrium Eq. (23) and boundary condition (25) reduce into;

$$
\begin{aligned}
&\left(\bar{A}\bar{h}\bar{r}\right)\frac{d^2\bar{u}}{d\bar{r}^2}+\left(\bar{A}\bar{r}\frac{d\bar{h}}{d\bar{r}}+\bar{A}\bar{h}\right)\frac{d\bar{u}}{d\bar{r}}+\left(\left(\bar{B}\frac{d\bar{h}}{d\bar{r}}\right)-\frac{1}{\bar{r}}\bar{A}\bar{h}\right)\bar{u}\\
&-\frac{r_o}{u_o}\alpha\Delta T_o\bar{r}\left(\frac{d\bar{h}}{d\bar{r}}\bar{C}\right)\left(\bar{\alpha}\Delta\bar{T}\right)-\frac{r_o}{u_o}\alpha\Delta T_o\left(\bar{h}\bar{C}\bar{r}\right)\frac{d\left(\bar{\alpha}\Delta\bar{T}\right)}{d\bar{r}}+\frac{r_o}{u_o}\bar{\gamma}\bar{\rho}\bar{r}^2\bar{h}=0
\end{aligned}
\tag{26}
$$

and

$$\bar{A}\frac{d\bar{u}}{d\bar{r}}+\bar{B}\frac{\bar{u}}{\bar{r}}-\frac{r_o}{u_o}\alpha\Delta T_o\bar{C}\left(\bar{\alpha}\Delta\bar{T}\right)=\frac{r_o}{u_o}\left(\bar{\tilde{\sigma}}_r\right) \qquad @\bar{r}=\bar{r}_i,1 \tag{27}$$

According to Ref. [68], the temperature distribution in a disk with variable thickness may be obtained by solving the following differential equation;

$$\bar{r}\bar{h}\bar{k}\frac{d^2\Delta\bar{T}}{d\bar{r}^2}+\left(\bar{h}\bar{k}+\bar{r}\bar{k}\frac{d\bar{h}}{d\bar{r}}\right)\frac{d\Delta\bar{T}}{d\bar{r}}=0 \tag{28}$$

where $\bar{k}$ is the non-dimensional thermal conductivity coefficient. Many authors have used Eq. (28) to represent the heat distribution in cylindrical coordinate [69-72]. Due to complexity of the governing differential equations and boundary conditions, they are solved using numerical schemes.

3. Results and discussion

Thermoelastic analysis of a nanodisk of variable thickness is performed based on strain gradient theory, in this section. The influences of various parameters such as thickness profile and temperature on the radial displacement and stresses are studied.

In this paper, mechanical properties of nanodisk are constant;

$$p(r)=p_o=\text{Constant} \tag{29}$$

where p_o is the material property at each radius. Nickel is considered for the material properties. Also, the nanodisk has variable thickness.

$$h(r)=\frac{h_o}{r^m} \tag{30}$$

In order to find the influence of temperature and angular velocity on radial displacements, radial and circumferential stresses, the following values given in Table 1 and 2 were assigned for the length scale material parameters [73] and mechanical properties [74] of the nanodisk, respectively. To deduce the results, it was assumed that the temperatures at the inner and outer radii are 25 °C and 100 °C, while the nanodisk angular velocity is *100 Rad/s*.

Table 1. The length scale material parameters a_i [73]

	material	a_1	a_2	a_3	a_4	a_5
1	Ni	0.2386	0.0134	0.0013	0.0934	0.2462
2	Cu	0.1833	0.0103	0.0010	0.0717	0.1891
3	Ag	0.1766	0.0269	0.0121	0.0376	0.0976
4	Au	0.2994	0.0944	0.0458	0.0312	0.1046
5	Al	0.1407	0.0027	-0.0083	0.0966	0.2584

Table 2. Mechanical property of materials [74]

	material	E (GPa)	υ	α $\mu m/(m\text{-}^\circ C)$	ρ (Kg/m^3)	$W/m-K$
1	Ni	207	0.31	13.1	8880	60.7
2	Cu	110	0.343	20.2	7764	483
3	Ag	76	0.37	19.9	10491	419
4	Au	77.2	0.42	14.6	19320	301
5	Al	68	0.36	25.5	2698.9	210

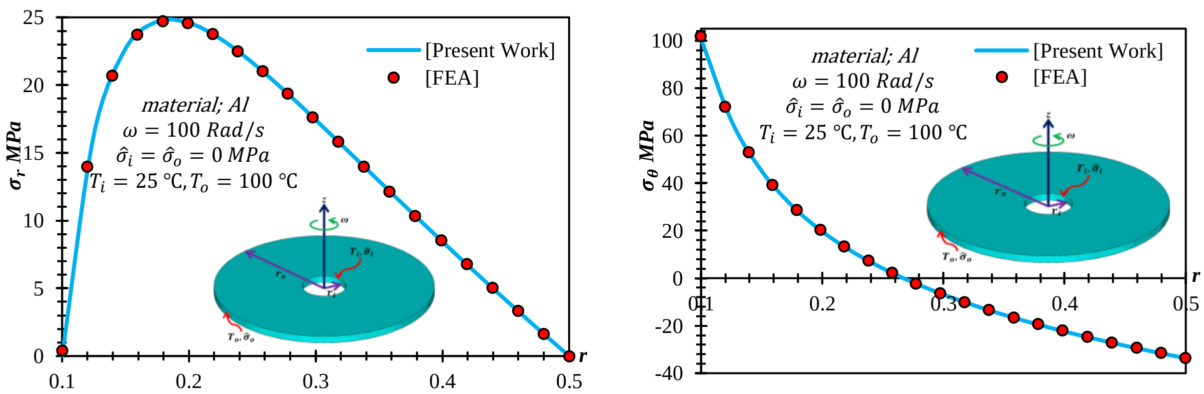

(a) Radial stress component. **(b)** Tangential stress component.

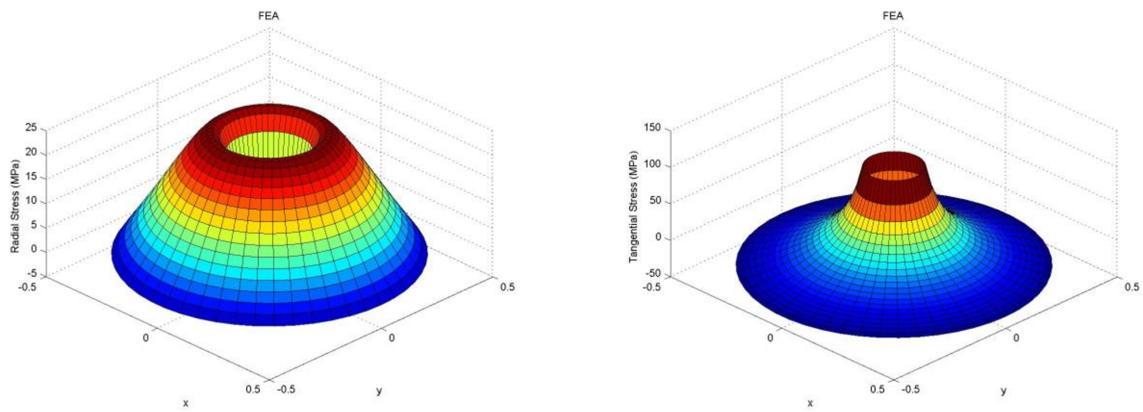

(a) Distribution of σ_r based on FE model **(b)** Distribution of σ_θ base on FE model

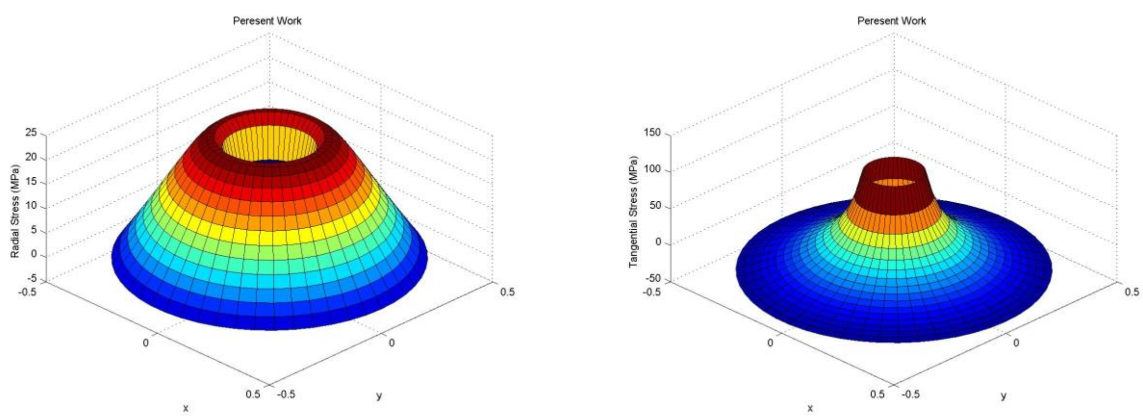

(c) Distribution of σ_r based on strain gradient theory **(d)** Distribution of σ_θ based on strain gradient theory

Fig. 2. Comparison between classical and strain gradient theory for a disk with thermal effect, (a) radial stresses (b) tangential stresses, (c) 3-D distribution of radial stresses obtained from FE results, (d) 3-D distribution of radial stresses obtained from FE results, (e) 3-D distribution of radial stresses using strain gradient theory, (f) 3-D distribution of tangential stresses using strain gradient theory.

Additionally, Fig. 2 illustrates radial and tangential stress components developed in a rotating disk based on current solution and those of finite element model. The finite element results are based on classical solution. Here, there is a variation in temperature which occurs along the macro-disk radius. As observed, the results based on the strain gradient theory match those of finite element solution at all points along the disk radius.

3.1. The effect of temperature

Fig. 3-7 present the effects of temperature on radial displacement and the induced stress components. It is noticed that angular velocity of the nanodisk was equal to 100 Rad/s and the external pressures were assumed to be zero at the inner and outer radii, in this section.

Fig. 3 displays the effect of temperature rise at the outer radius on the induced radial stress, based on strain gradient theory. This results show that the location of zero induced radial stress $\bar{\sigma}_r$ remains intact at $\bar{r}$=0.91. Maximum values of radial stresses occurred at inner radius for all values of temperature.

Depicted in Fig. 4 is the influence of temperature variation on non-dimensional circumferential stress $\bar{\sigma}_\theta$. This figure shows that zero circumferential stress occurs at $\bar{r}$=0.5 for all values of T_o. Also, the outer radius is more affected by the induced temperature profile.

The effect of temperature rising at outer radius on the high-order stresses plotted in Fig. 5-7. As it is seen, non-dimensional high-order stresses, $\bar{\tau}_{rrr}$, $\bar{\tau}_{\theta\theta r}$ and $\bar{\tau}_{r\theta\theta}$ have positive relation to temperature. Also, these figures show that the location of maximum values (maximum values location) of $\bar{\tau}_{rrr}$, $\bar{\tau}_{\theta\theta r}$ and $\bar{\tau}_{r\theta\theta}$ occurred at fixed points. So, it can conclude that the location of maximum values (maximum values location) of high-order stresses are not dependent on temperature rising. Reminder that $\bar{\tau}_{rrr}$ is one of the boundary conditions. Fig. 5 demonstrates that due to zero boundary condition (applied mechanical boundary condition in this section), the values of $\bar{\tau}_{rrr}$ are zero at boundaries and the boundary conditions are satisfied.

To show the effect of temperature rising, variation of total stresses versus the non-dimensional radius are plotted in Fig. 8 and 9. Total non-dimensional stresses have positive relation to temperature. Location of maximum values (maximum values location) of total stresses are independent of temperature. Note that unlike classical elasticity theory, $\bar{\sigma}_r$ or $\bar{\sigma}_r^t$ isn't a boundary condition. Therefore, as shown in Fig. 8, $\bar{\sigma}_r^t$ isn't equal to zero, while applied external load are equal to zero at boundaries. Total tangential stresses are equal to zero at $\bar{r}$ ≈0.47 for all temperatures at outer radii. Note that the total radial and tangential stresses increasing as T_o increasing.

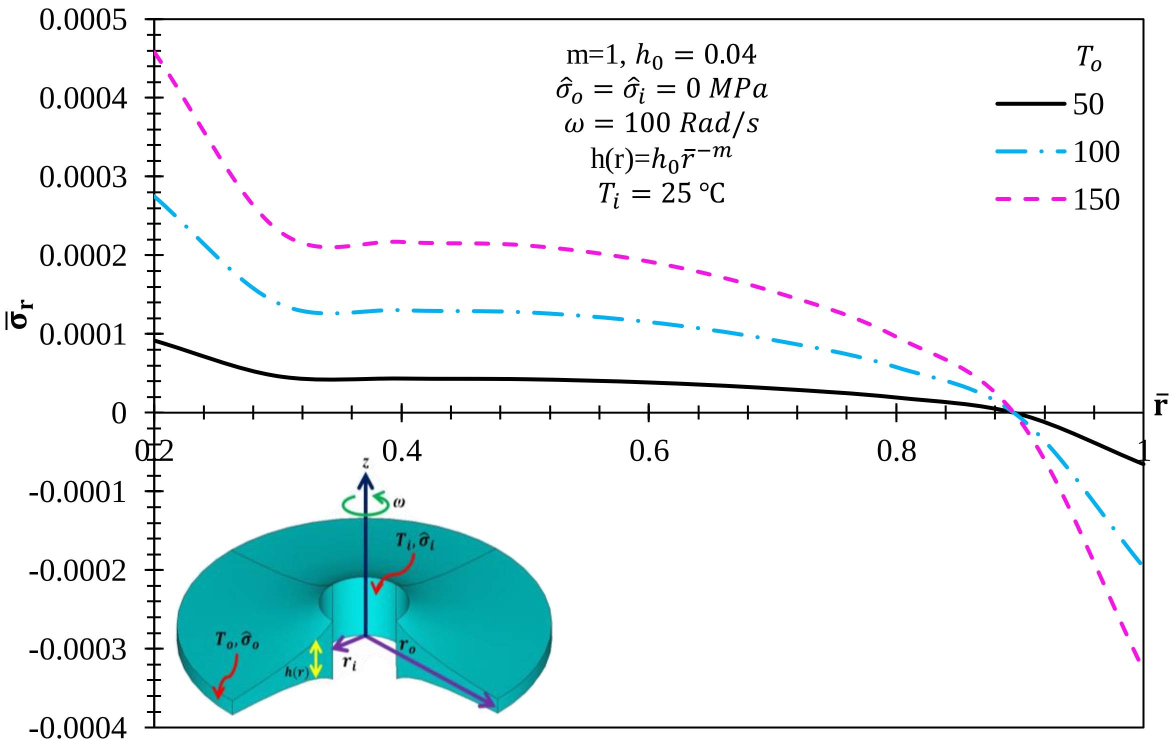

Fig. 3. The effect of temperature profile on dimensionless radial stress.

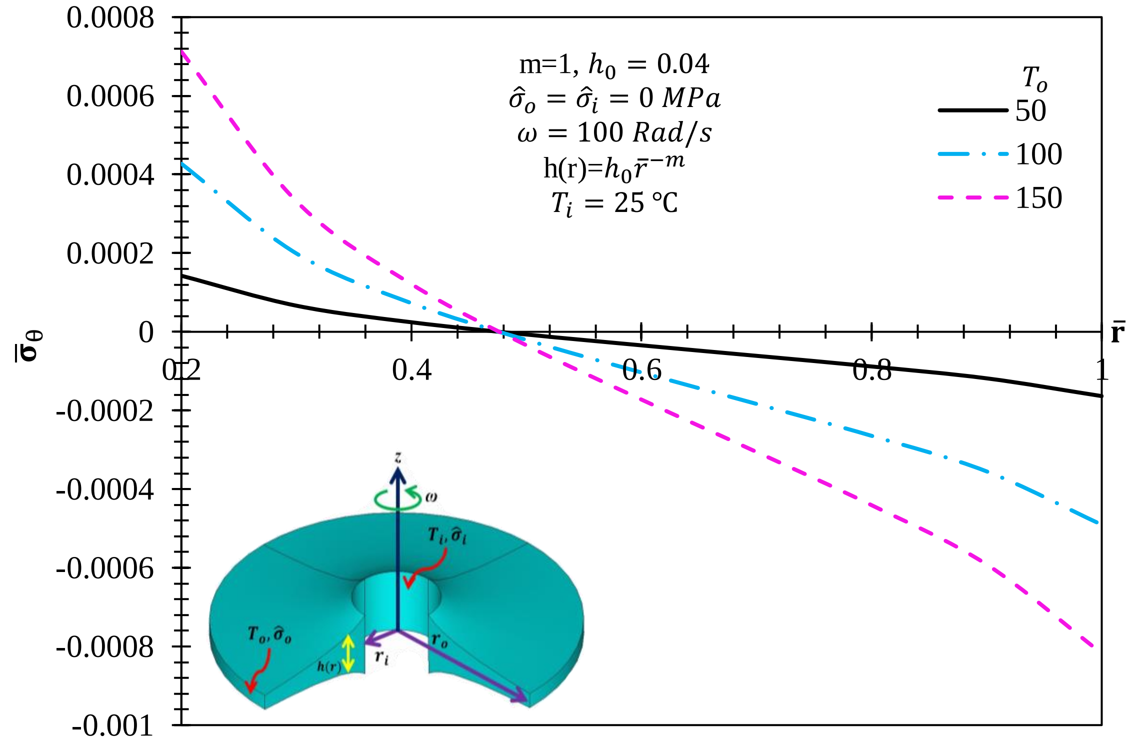

Fig. 4. The effect of temperature profiles on dimensionless circumferential stress.

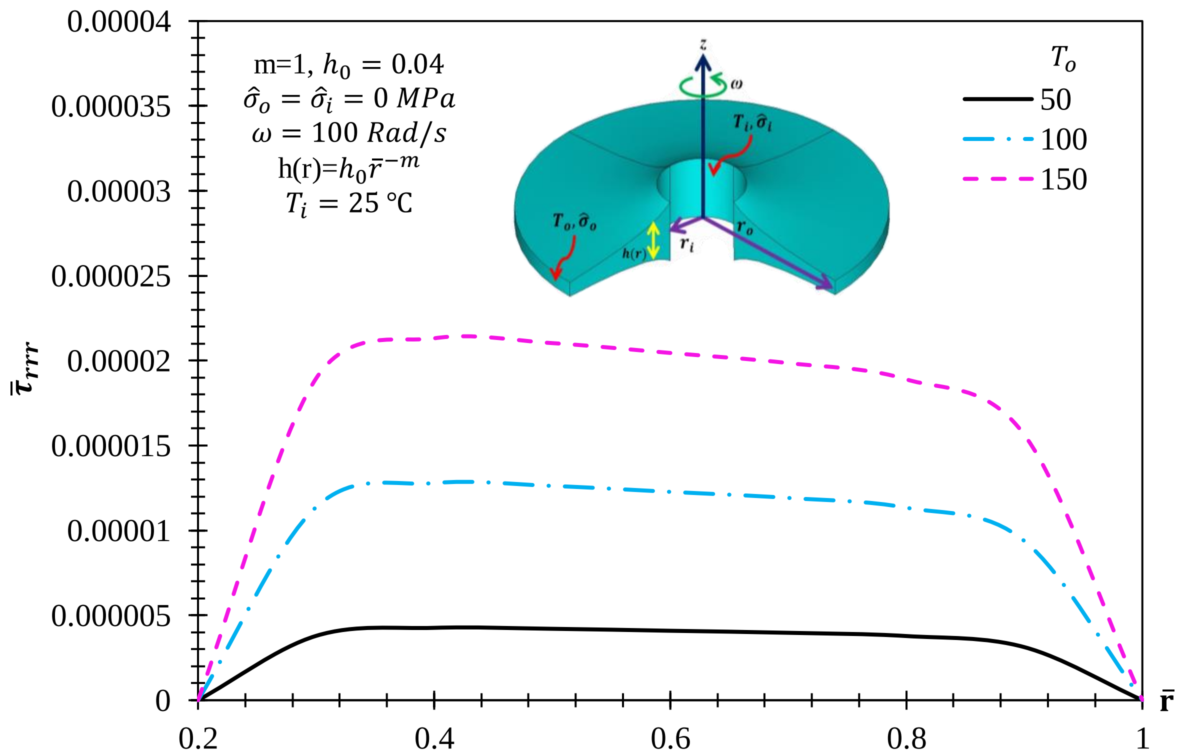

Fig. 5. The effect of temperature profiles on $\bar{\tau}_{rrr}$.

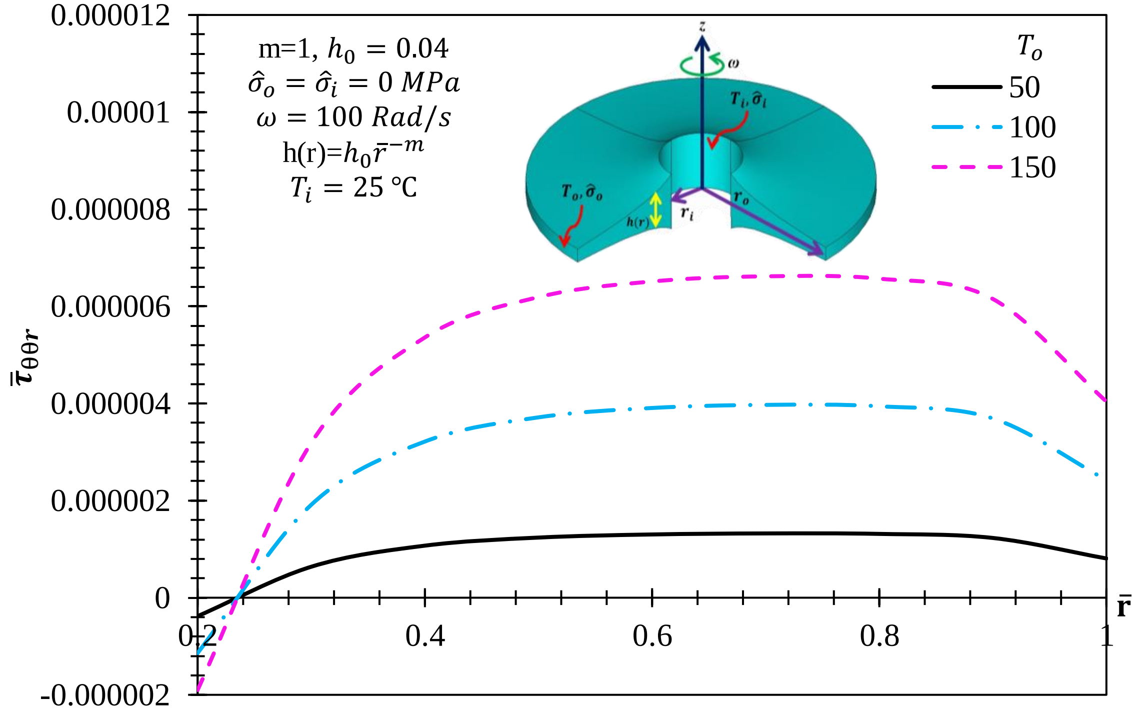

Fig. 6. The effect of temperature profiles on $\bar{\tau}_{\theta\theta r}$.

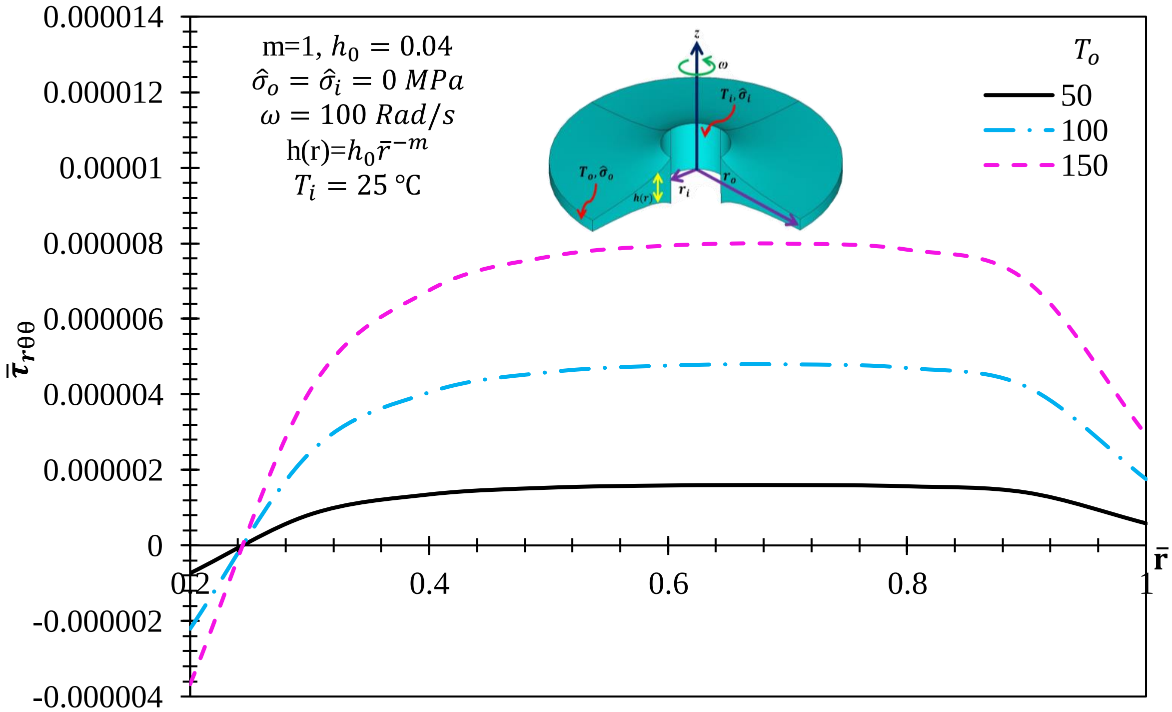

Fig. 7. The effect of temperature profiles on $\bar{\tau}_{r\theta\theta}$.

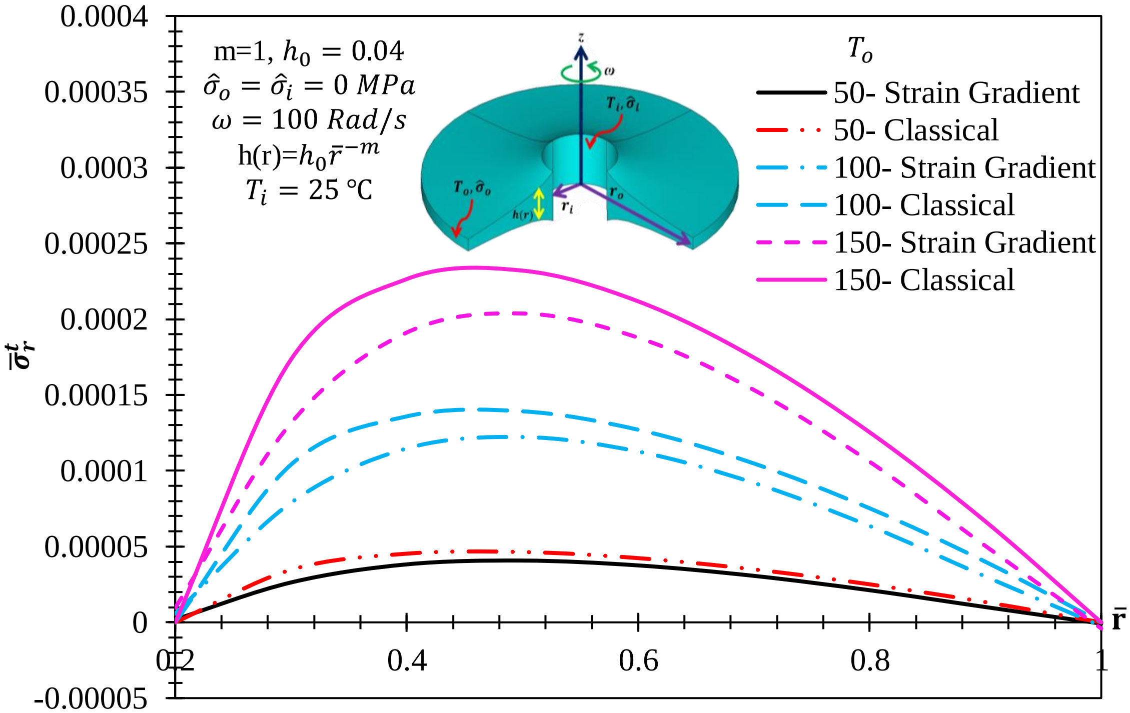

Fig. 8. The effect of temperature profile on the $\bar{\sigma}_r^t$.

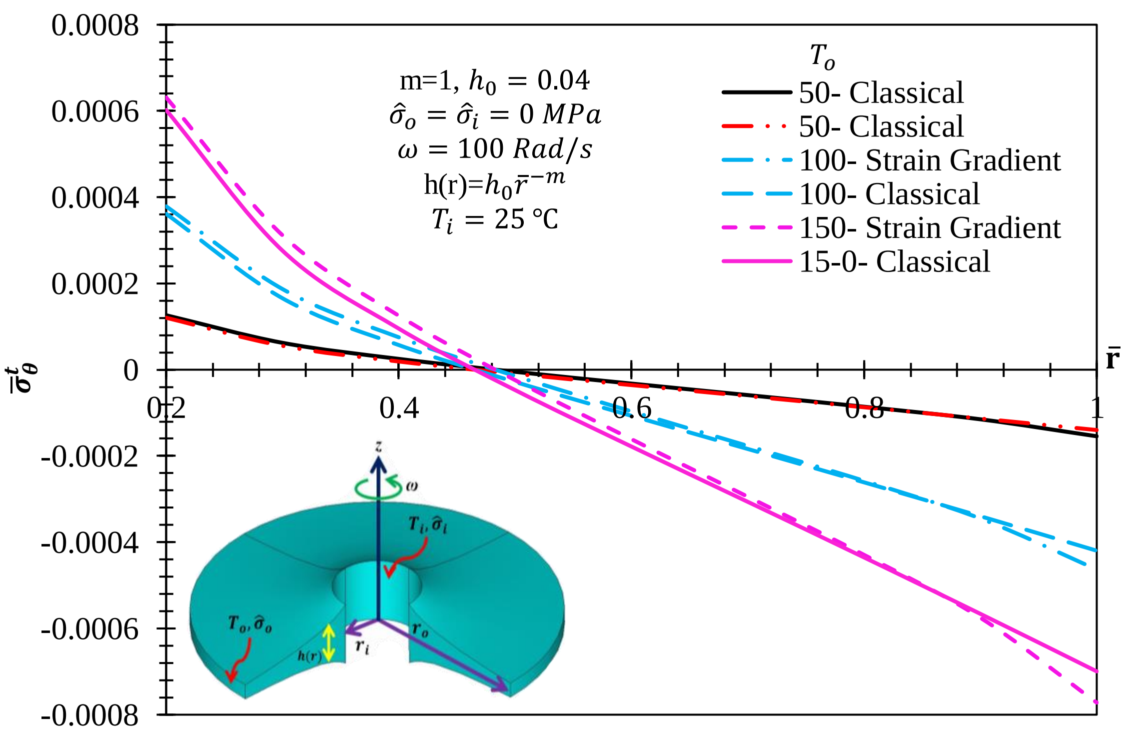

Fig. 9. The effect of temperature profile on the $\bar{\sigma}_\theta^t$.

3.2. The effect of thickness profile

The thickness profiles for different values of m are plotted in Fig. 10. The thickness at inner radius increases as m increases, while the thickness of nanodisk at outer radius is constant. Fig. 11 explain the distribution of $\Delta\bar{T}$ along the radius of nanodisk for different thicknesses and temperature variation decreases with increasing m. So, it is predicted that we can obtained better stress distribution along radius of nanodisk for larger amounts of m.

Plotted in Fig. 12 is the influence of thickness profile on the radial displacement. It is clearly seen from this figure that the radial displacements decreasing as m increasing. Therefore, it is concluded that the variable thickness is better than constant thickness for nanodisk under thermal and mechanical loads. Due to angular velocity and greater temperature at outer radius, radial displacements at outer radiuses are greater than radial displacements at inner radiuses (radial displacement curve are ascending).

Fig. 13 and 14 depict the effects of thickness profile on the non-dimensional radial and tangential stresses. As m increases, stresses decrease and increase at inner and outer radii, respectively. Radial stresses have same value at $\bar{r}$=0.9 for all values of m.

Fig. 15-17 show the non-dimensional high-order stresses for different thickness profiles. It is clearly observed from these figures that the location of maximum of high-order stresses and the maximum values of high-order stresses are depend on m, in this case. The use of variable thickness decreases the maximum values of high-order stress $\bar{\tau}_{rrr}$.

Fig. 18 and 19 present the distribution of total radial and tangential stresses along radius of nanodisk for different thickness profiles. Again it is seen that total radial stresses are nonzero at inner and outer radius, while the external loads at boundaries are zero. The use of variable thickness can be reduced total radial stress, and maximum total radial stress location depend on thickness profile. But it should be noted that the use of variable thickness increased circumferential stress at outer radii of nanodisk.

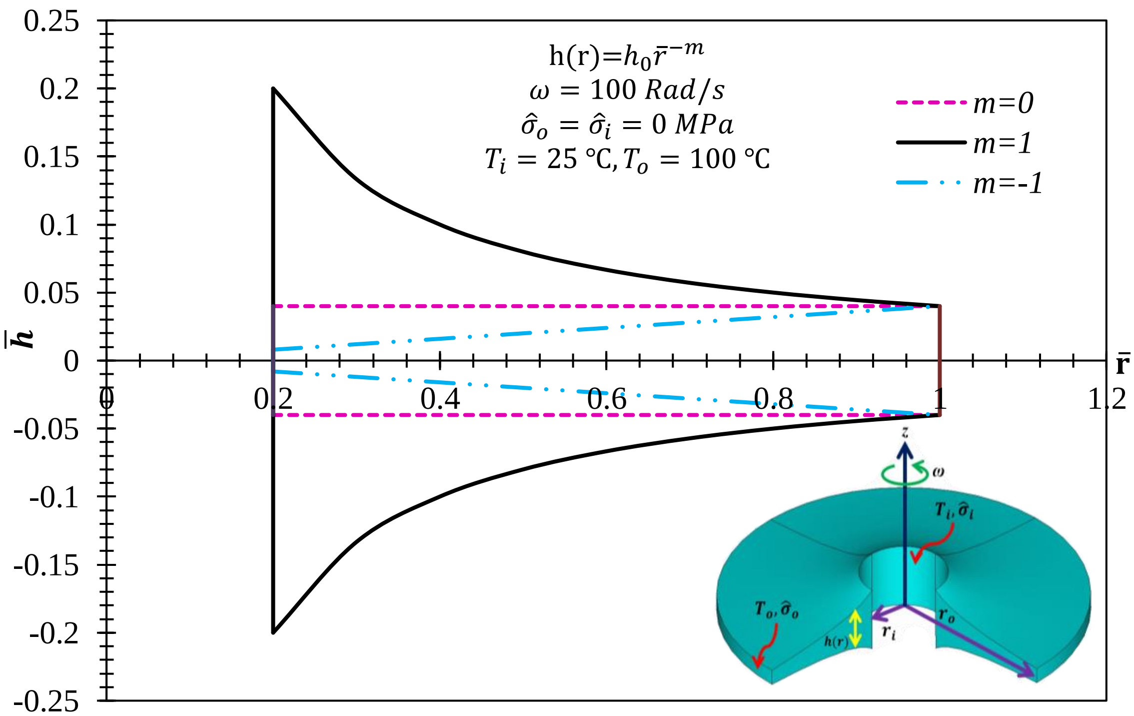

Fig. 10. Thickness profile for different values of *m*.

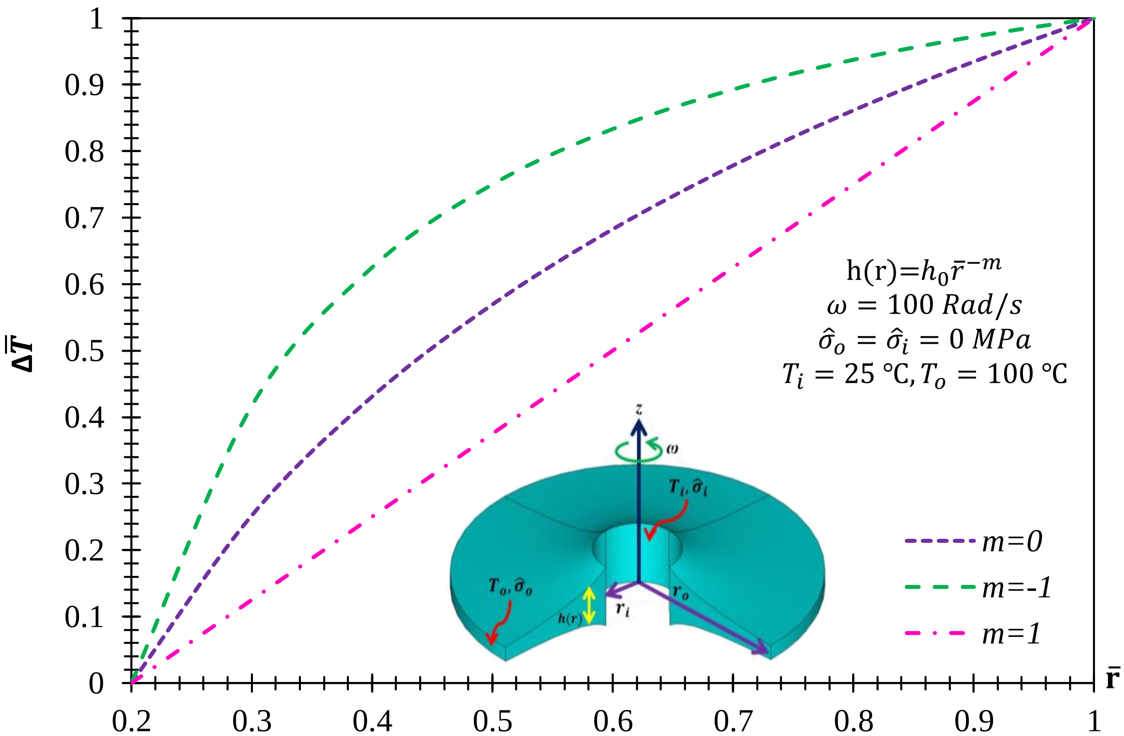

Fig. 11. The effect of thickness profiles on the temperature distribution.

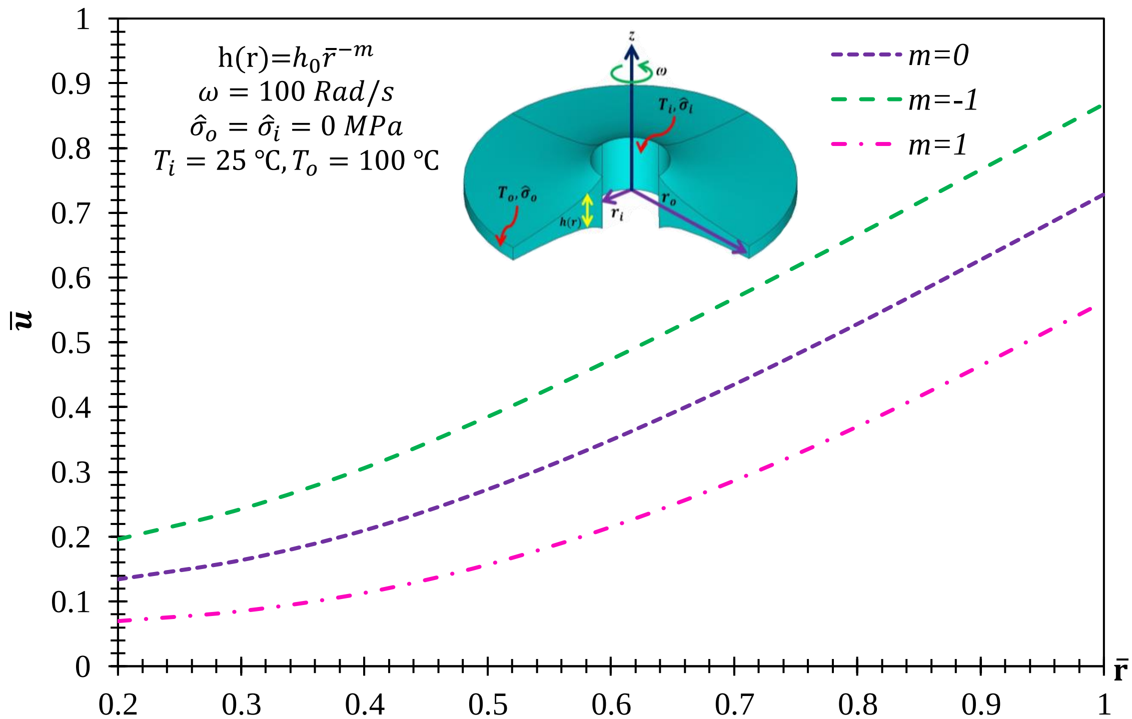

Fig. 12. The effect of thickness profile on dimensionless radial displacement.

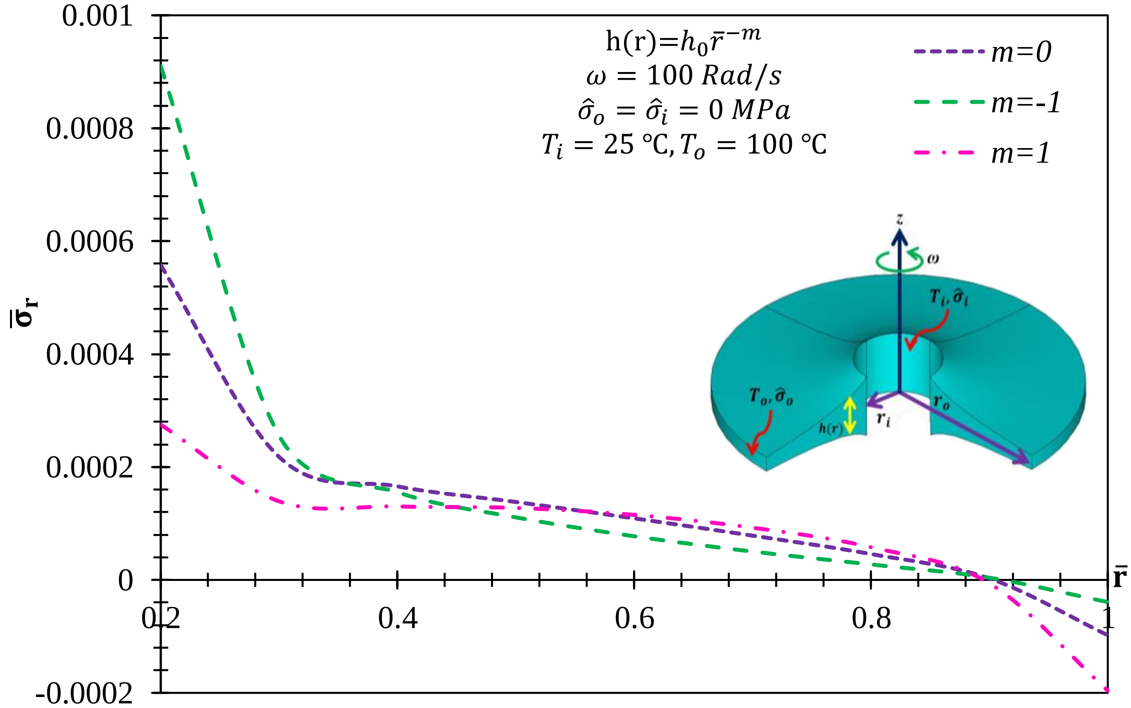

Fig. 13. The effect of thickness profile on dimensionless radial stress.

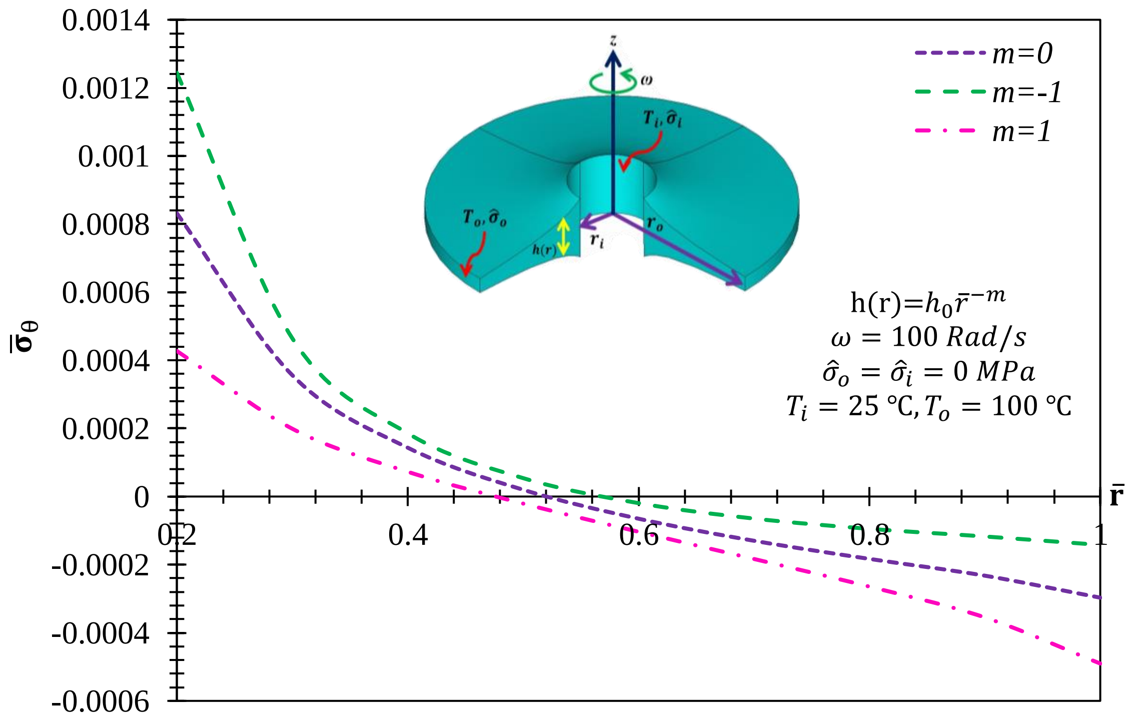

Fig. 14. The effect of thickness profile on dimensionless circumferential stress.

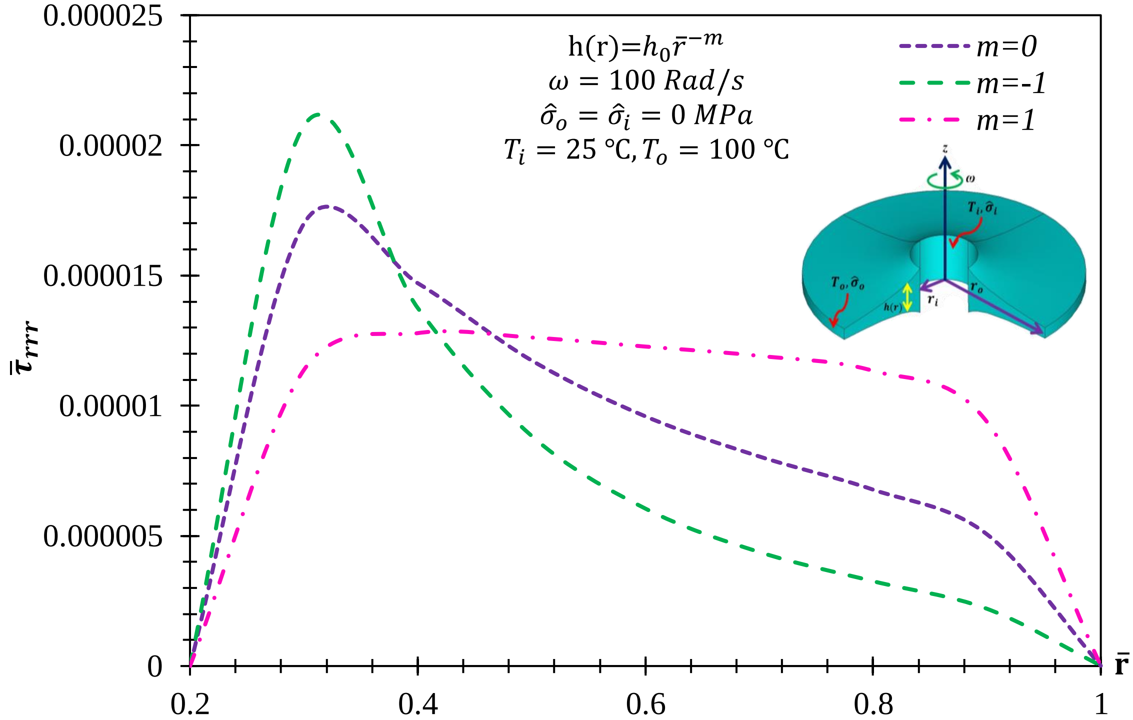

Fig. 15. The effect of thickness profile on $\bar{\tau}_{rrr}$.

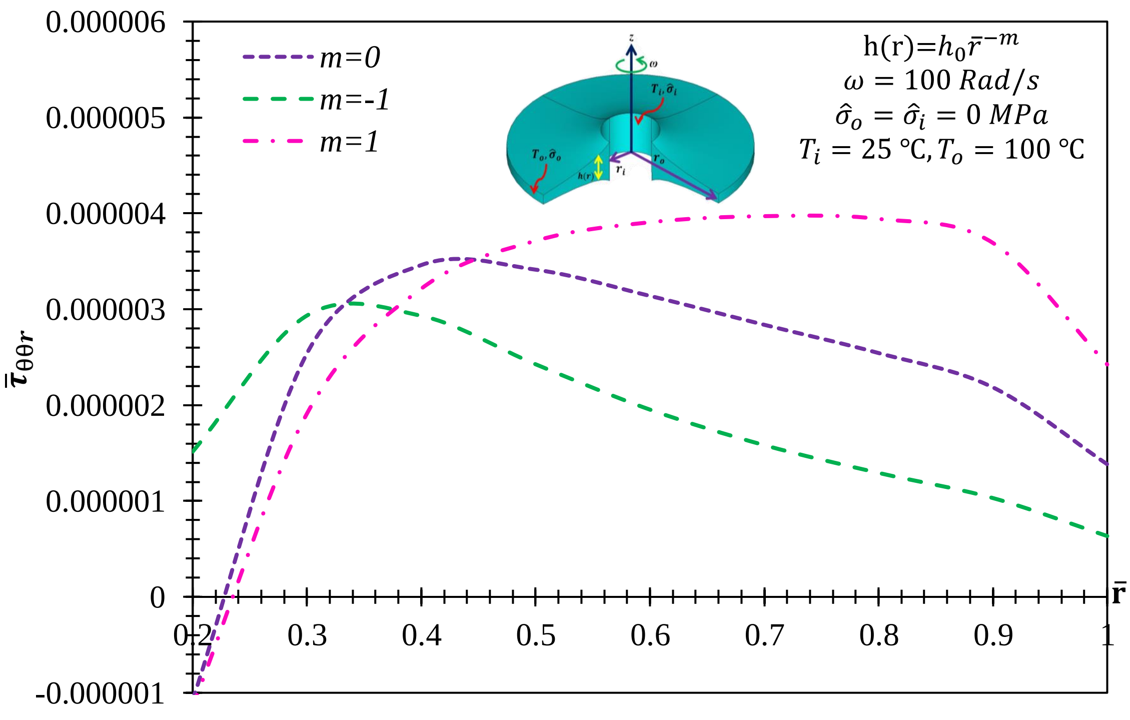

Fig. 16. The effect of thickness profile on $\bar{\tau}_{\theta\theta r}$..

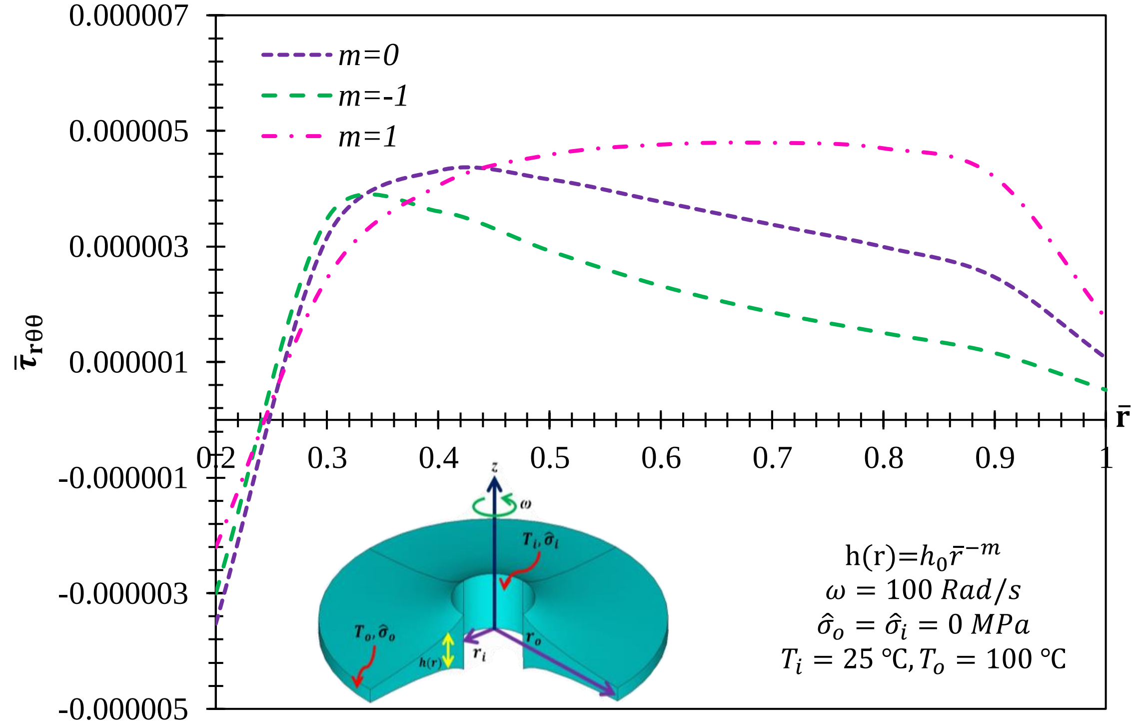

Fig. 17. The effect of thickness profile on $\bar{\tau}_{r\theta\theta}$.

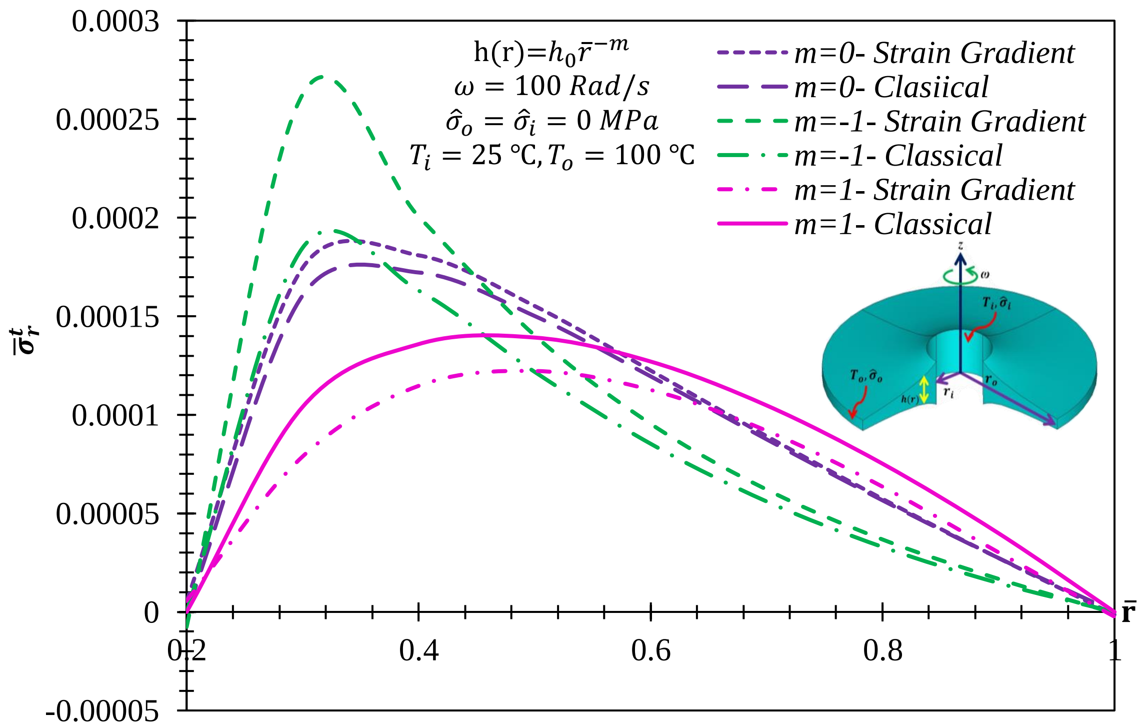

Fig. 18. The effect of thickness profile on $\bar{\sigma}_r^t$.

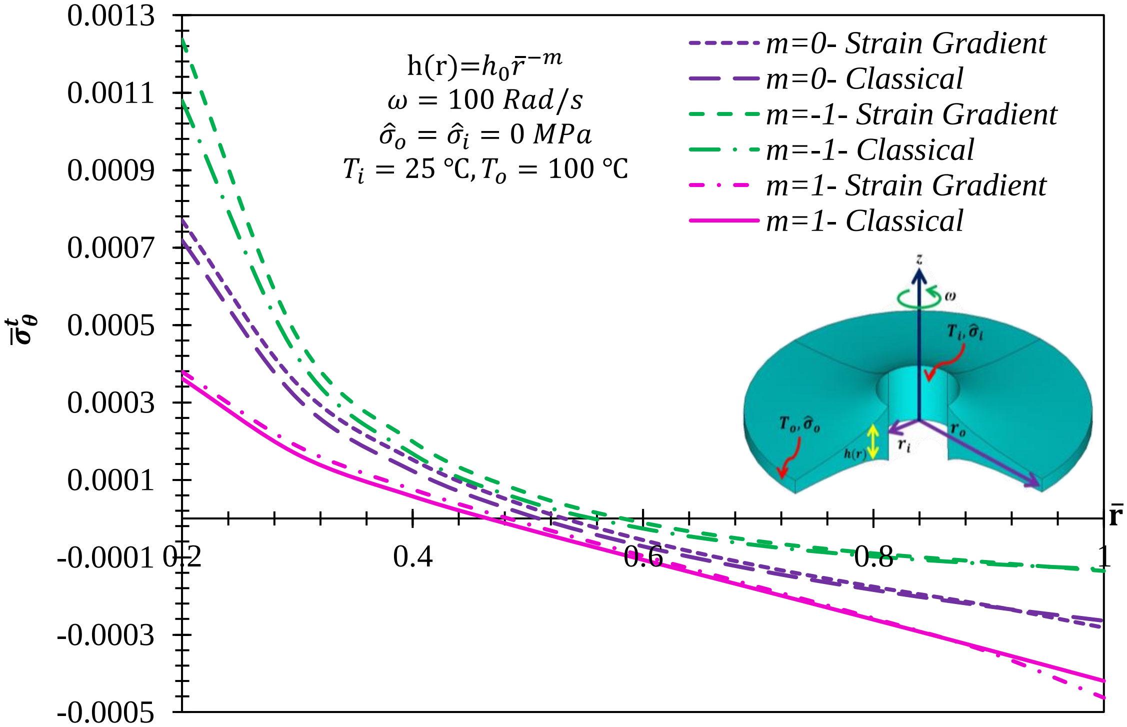

Fig. 19. The effect of thickness profile on $\bar{\sigma}_\theta^t$.

3.3. The effect of angular velocity

Finally, Table 3 is presented to compare total radial stress, $\bar{\sigma}_r^t$, for different angular velocities, ω. The results show that for moderate values of angular velocity, total radial stress are barely affected. Due to a very small radius, the centrifugal force is negligible. Therefore, this result seems reasonable due to the very small radius.

Table 3. The effect of angular velocity on the total non-dimensional radial stress ($\times 10^{-5}$)

$\bar{r}$	ω				
	0	10^2	10^5	10^8	10^{10}
0.2	0.570078	0.570078	0.570078	0.570081	0.595948
0.3	7.88574	7.88574	7.88574	7.88575	8.0253
0.4	11.4694	11.4694	11.4694	11.4694	11.6606
0.5	12.2243	12.2243	12.2243	12.2243	12.4339
0.6	11.2664	11.2664	11.2664	11.2664	11.4706
0.7	9.19595	9.19595	9.19595	9.19596	9.37528
0.8	6.35429	6.35429	6.35429	6.3543	6.49103
0.9	3.02204	3.02204	3.02204	3.02205	3.09953
1	-0.24309	-0.243085	-0.243085	-0.243085	-0.242199

4. Conclusions

In this paper, thermoelastic analysis of a rotating nanodisk with non-uniform thickness based on strain gradient theory is presented. Numerical results show that use of nanodisk with variable thickness is more appropriate. Main findings are;

1- Results show that we can control stresses by using variable thickness.
2- Temperature at outside radius has a direct effect on radial displacement of nanodisk. It is seen that the location of maximum high-order stresses is not affected by temperature and the location of peak high-order stresses depend on *m*, only.
3- Additionally, any change in the temperature profile within the nanodisk (in terms of any increase in the temperature at the outer radius) has a direct effect on radial displacements as well as induced stresses along the nanodisk radius. The radial displacement increases as the temperatures at outer radii increases. On the other hand, results indicate that it can reduce total radial stress and maximum total radial stress location by using variable thickness.

5. References

[1] M. Hosseini, M. Shishesaz, A. Hadi, Thermoelastic analysis of rotating functionally graded micro/nanodisks of variable thickness, *Thin-Walled Structures*, Vol. 134, pp. 508-523, 2019.

[2] K. Q. d. Costa, V. Dmitriev, Comparative analysis of circular and triangular gold nanodisks for field enhancement applications, *Journal of Microwaves, Optoelectronics and Electromagnetic Applications*, Vol. 9, No. 2, pp. 123-130, 2010.

[3] E. D. Williams, Nanoscale structures: Lability, length scales, and fluctuations, *MRS bulletin*, Vol. 29, No. 09, pp. 621-629, 2004.

[4] M. Farajpour, A. Shahidi, A. Hadi, A. Farajpour, Influence of initial edge displacement on the nonlinear vibration, electrical and magnetic instabilities of magneto-electro-elastic nanofilms, *Mechanics of Advanced Materials and Structures*, Vol. 26, No. 17, pp. 1469-1481, 2019.

[5] M. Mohammadi, M. Hosseini, M. Shishesaz, A. Hadi, A. Rastgoo, Primary and secondary resonance analysis of porous functionally graded nanobeam resting on a nonlinear foundation subjected to mechanical and electrical loads, *European Journal of Mechanics-A/Solids*, Vol. 77, pp. 103793, 2019.

[6] E. Zarezadeh, V. Hosseini, A. Hadi, Torsional vibration of functionally graded nano-rod under magnetic field supported by a generalized torsional foundation based on nonlocal elasticity theory, *Mechanics Based Design of Structures and Machines*, pp. 1-16, 2019.

[7] A. Soleimani, K. Dastani, A. Hadi, M. H. Naei, Effect of out-of-plane defects on the postbuckling behavior of graphene sheets based on nonlocal elasticity theory, *Steel and Composite Structures*, Vol. 30, No. 6, pp. 517-534, 2019.

[8] A. Hadi, A. Rastgoo, N. Haghighipour, A. Bolhassani, Numerical modelling of a spheroid living cell membrane under hydrostatic pressure, *Journal of Statistical Mechanics: Theory and Experiment*, Vol. 2018, No. 8, pp. 083501, 2018.

[9] M. Z. Nejad, A. Hadi, A. Omidvari, A. Rastgoo, Bending analysis of bi-directional functionally graded Euler-Bernoulli nano-beams using integral form of Eringen's non-local elasticity theory, *Structural Engineering and Mechanics*, Vol. 67, No. 4, pp. 417-425, 2018.

[10] A. Hadi, M. Z. Nejad, M. Hosseini, Vibrations of three-dimensionally graded nanobeams, *International Journal of Engineering Science*, Vol. 128, pp. 12-23, 2018.

[11] M. Hosseini, A. Hadi, A. Malekshahi, M. Shishesaz, A review of size-dependent elasticity for nanostructures, *Journal of Computational Applied Mechanics*, Vol. 49, No. 1, pp. 197-211, 2018.

[12] A. Hadi, M. Z. Nejad, A. Rastgoo, M. Hosseini, Buckling analysis of FGM Euler-Bernoulli nano-beams with 3D-varying properties based on consistent couple-stress theory, *Steel and Composite Structures*, Vol. 26, No. 6, pp. 663-672, 2018.

[13] M. Shishesaz, M. Hosseini, K. N. Tahan, A. Hadi, Analysis of functionally graded nanodisks under thermoelastic loading based on the strain gradient theory, *Acta Mechanica*, Vol. 228, No. 12, pp. 4141-4168, 2017.

[14] M. Hosseini, H. H. Gorgani, M. Shishesaz, A. Hadi, Size-dependent stress analysis of single-wall carbon nanotube based on strain gradient theory, *International Journal of Applied Mechanics*, Vol. 9, No. 06, pp. 1750087, 2017.

[15] M. M. Adeli, A. Hadi, M. Hosseini, H. H. Gorgani, Torsional vibration of nano-cone based on nonlocal strain gradient elasticity theory, *The European Physical Journal Plus*, Vol. 132, No. 9, pp. 393, 2017.

[16] M. Z. Nejad, A. Hadi, A. Farajpour, Consistent couple-stress theory for free vibration analysis of Euler-Bernoulli nano-beams made of arbitrary bi-directional functionally graded materials, *Structural Engineering and Mechanics*, Vol. 63, No. 2, pp. 161-169, 2017.

[17] M. Hosseini, M. Shishesaz, K. N. Tahan, A. Hadi, Stress analysis of rotating nano-disks of variable thickness made of functionally graded materials, *International Journal of Engineering Science*, Vol. 109, pp. 29-53, 2016.

[18] M. Z. Nejad, A. Hadi, Non-local analysis of free vibration of bi-directional functionally graded Euler–Bernoulli nano-beams, *International Journal of Engineering Science*, Vol. 105, pp. 1-11, 2016/08/01/, 2016.

[19] M. Z. Nejad, A. Hadi, Eringen's non-local elasticity theory for bending analysis of bi-directional functionally graded Euler–Bernoulli nano-beams, *International Journal of Engineering Science*, Vol. 106, pp. 1-9, 2016/09/01/, 2016.

[20] M. Z. Nejad, A. Hadi, A. Rastgoo, Buckling analysis of arbitrary two-directional functionally graded Euler–Bernoulli nano-beams based on nonlocal elasticity theory, *International Journal of Engineering Science*, Vol. 103, pp. 1-10, 2016.

[21] M. Shishesaz, M. Hosseini, Mechanical behavior of functionally graded nano-cylinders under radial pressure based on strain gradient theory, *Journal of Mechanics*, Vol. 35, No. 4, pp. 441-454, 2019.

[22] R. Noroozi, A. Barati, A. Kazemi, S. Norouzi, A. Hadi, Torsional vibration analysis of bi-directional FG nano-cone with arbitrary cross-section based on nonlocal strain gradient elasticity.

[23] M. M. Khoram, M. Hosseini, A. Hadi, M. Shishehsaz, Bending Analysis of Bi-Directional FGM Timoshenko Nano-Beam subjected to mechanical and magnetic forces and resting on Winkler-Pasternak foundation, Vol. 0, No. ja, pp. null.

[24] M. M. Khoram, M. Hosseini, A. Hadi, M. Shishehsaz, Bending Analysis of Bi-Directional FGM Timoshenko Nano-Beam subjected to mechanical and magnetic forces and resting on Winkler-Pasternak foundation, *International Journal of Applied Mechanics*, 2020.

[25] A. Barati, M. M. Adeli, A. Hadi, Static torsion of bi-directional functionally graded microtube based on the couple stress theory under magnetic field, *International Journal of Applied Mechanics*, Vol. 12, No. 02, pp. 2050021, 2020.

[26] A. M. Abazari, S. M. Safavi, G. Rezazadeh, L. G. Villanueva, Size Effects on Mechanical Properties of Micro/Nano Structures, *arXiv preprint arXiv:1508.01322*, 2015.

[27] A. Daneshmehr, A. Rajabpoor, A. Hadi, Size dependent free vibration analysis of nanoplates made of functionally graded materials based on nonlocal elasticity theory with high order theories, *International Journal of Engineering Science*, Vol. 95, pp. 23-35, 2015.

[28] A. C. Eringen, Nonlocal polar elastic continua, *International journal of engineering science*, Vol. 10, No. 1, pp. 1-16, 1972.

[29] A. C. Eringen, 2002, *Nonlocal continuum field theories*, Springer Science & Business Media,

[30] A. C. Eringen, Theory of micromorphic materials with memory, *International Journal of Engineering Science*, Vol. 10, No. 7, pp. 623-641, 1972.

[31] A. C. Eringen, On differential equations of nonlocal elasticity and solutions of screw dislocation and surface waves, *Journal of applied physics,* Vol. 54, No. 9, pp. 4703-4710, 1983.

[32] D. Lam, F. Yang, A. Chong, J. Wang, P. Tong, Experiments and theory in strain gradient elasticity, *Journal of the Mechanics and Physics of Solids,* Vol. 51, No. 8, pp. 1477-1508, 2003.

[33] R. A. Toupin, Elastic materials with couple-stresses, *Archive for Rational Mechanics and Analysis,* Vol. 11, No. 1, pp. 385-414, 1962.

[34] R. Mindlin, H. Tiersten, Effects of couple-stresses in linear elasticity, *Archive for Rational Mechanics and Analysis,* Vol. 11, No. 1, pp. 415-448, 1962.

[35] M. Najafzadeh, M. M. Adeli, E. Zarezadeh, A. Hadi, Torsional vibration of the porous nanotube with an arbitrary cross-section based on couple stress theory under magnetic field, *Mechanics Based Design of Structures and Machines*, pp. 1-15, 2020.

[36] R. Mindlin, N. Eshel, On first strain-gradient theories in linear elasticity, *International Journal of Solids and Structures,* Vol. 4, No. 1, pp. 109-124, 1968.

[37] M. R. Ghazavi, H. Molki, A. Ali beigloo, Nonlinear vibration and stability analysis of the curved microtube conveying fluid as a model of the micro coriolis flowmeters based on strain gradient theory, *Applied Mathematical Modelling*.

[38] L. Li, Y. Hu, Buckling analysis of size-dependent nonlinear beams based on a nonlocal strain gradient theory, *International Journal of Engineering Science,* Vol. 97, pp. 84-94, 12//, 2015.

[39] L. Li, X. Li, Y. Hu, Free vibration analysis of nonlocal strain gradient beams made of functionally graded material, *International Journal of Engineering Science,* Vol. 102, pp. 77-92, 5//, 2016.

[40] L. Li, Y. Hu, X. Li, Longitudinal vibration of size-dependent rods via nonlocal strain gradient theory, *International Journal of Mechanical Sciences,* Vol. 115–116, pp. 135-144, 9//, 2016.

[41] O. Rahmani, S. A. H. Hosseini, I. Ghoytasi, H. Golmohammadi, Buckling and free vibration of shallow curved micro/nano-beam based on strain gradient theory under thermal loading with temperature-dependent properties, *Applied Physics A,* Vol. 123, No. 1, pp. 4, 2016.

[42] A. Li, S. Zhou, L. Qi, Size-dependent electromechanical coupling behaviors of circular micro-plate due to flexoelectricity, *Applied Physics A,* Vol. 122, No. 10, pp. 918, 2016.

[43] F. Ebrahimi, M. R. Barati, Vibration analysis of viscoelastic inhomogeneous nanobeams incorporating surface and thermal effects, *Applied Physics A,* Vol. 123, No. 1, pp. 5, 2016//, 2016.

[44] F. Ebrahimi, M. R. Barati, Wave propagation analysis of quasi-3D FG nanobeams in thermal environment based on nonlocal strain gradient theory, *Applied Physics A,* Vol. 122, No. 9, pp. 843, 2016.

[45] Y. Zheng, T. Chen, C. Chen, A size-dependent model to study nonlinear static behavior of piezoelectric cantilever microbeams with damage, *Microsystem Technologies,* pp. 1-8, 2017//, 2017.

[46] F. Tavakolian, A. Farrokhabadi, Size-dependent dynamic instability of double-clamped nanobeams under dispersion forces in the presence of thermal stress effects, *Microsystem Technologies*, pp. 1-15, 2017//, 2017.

[47] K. Raahemifar, Size-dependent asymmetric buckling of initially curved shallow nano-beam using strain gradient elasticity, *Microsystem Technologies*, pp. 1-12, 2017//, 2017.

[48] M. Soltanpour, M. Ghadiri, A. Yazdi, M. Safi, Free transverse vibration analysis of size dependent Timoshenko FG cracked nanobeams resting on elastic medium, *Microsystem Technologies*, pp. 1-18, 2016//, 2016.

[49] M. H. Ghayesh, H. Farokhi, A. Gholipour, S. Hussain, Complex motion characteristics of three-layered Timoshenko microarches, *Microsystem Technologies*, pp. 1-14, 2016//, 2016.

[50] A. Soleimani, M. H. Naei, M. M. Mashhadi, Buckling analysis of graphene sheets using nonlocal isogeometric finite element method for NEMS applications, *Microsystem Technologies*, pp. 1-13, 2016//, 2016.

[51] M. H. Ghayesh, H. Farokhi, S. Hussain, A. Gholipour, M. Arjomandi, A size-dependent nonlinear third-order shear-deformable dynamic model for a microplate on an elastic medium, *Microsystem Technologies*, pp. 1-19, 2016//, 2016.

[52] M. E. Golmakani, H. Vahabi, Nonlocal buckling analysis of functionally graded annular nanoplates in an elastic medium with various boundary conditions, *Microsystem Technologies*, pp. 1-16, 2016//, 2016.

[53] J. S. Peng, L. Yang, J. Yang, Size effect on the dynamic analysis of electrostatically actuated micro-actuators, *Microsystem Technologies*, pp. 1-8, 2015//, 2015.

[54] R. Ansari, M. Faraji Oskouie, H. Rouhi, Studying linear and nonlinear vibrations of fractional viscoelastic Timoshenko micro-/nano-beams using the strain gradient theory, *Nonlinear Dynamics,* Vol. 87, No. 1, pp. 695-711, 2017//, 2017.

[55] R. Gholami, R. Ansari, A most general strain gradient plate formulation for size-dependent geometrically nonlinear free vibration analysis of functionally graded shear deformable rectangular microplates, *Nonlinear Dynamics,* Vol. 84, No. 4, pp. 2403-2422, 2016.

[56] V. Mohammadi, R. Ansari, M. Faghih Shojaei, R. Gholami, S. Sahmani, Size-dependent dynamic pull-in instability of hydrostatically and electrostatically actuated circular microplates, *Nonlinear Dynamics,* Vol. 73, No. 3, pp. 1515-1526, 2013//, 2013.

[57] S. Ramezani, Nonlinear vibration analysis of micro-plates based on strain gradient elasticity theory, *Nonlinear Dynamics,* Vol. 73, No. 3, pp. 1399-1421, 2013//, 2013.

[58] R. Ansari, H. Ramezannezhad, R. Gholami, Nonlocal beam theory for nonlinear vibrations of embedded multiwalled carbon nanotubes in thermal environment, *Nonlinear Dynamics,* Vol. 67, No. 3, pp. 2241-2254, 2012//, 2012.

[59] S. Zaitsev, O. Shtempluck, E. Buks, O. Gottlieb, Nonlinear damping in a micromechanical oscillator, *Nonlinear Dynamics,* Vol. 67, No. 1, pp. 859-883, 2012//, 2012.

[60] H. Sumali, M. I. Younis, E. M. Abdel-Rahman, Special issue on micro- and nano-electromechanical systems, *Nonlinear Dynamics,* Vol. 54, No. 1, pp. 1-2, 2008//, 2008.

[61] Y. Wang, F.-M. Li, Y.-Z. Wang, Nonlocal effect on the nonlinear dynamic characteristics of buckled parametric double-layered nanoplates, *Nonlinear Dynamics,* Vol. 85, No. 3, pp. 1719-1733, 2016//, 2016.

[62] K. Kiani, Nonlinear vibrations of a single-walled carbon nanotube for delivering of nanoparticles, *Nonlinear Dynamics,* Vol. 76, No. 4, pp. 1885-1903, 2014.

[63] H. Mohammadi, M. Mahzoon, M. Mohammadi, M.

Mohammadi, Postbuckling instability of nonlinear nanobeam with geometric imperfection embedded in elastic foundation, *Nonlinear Dynamics*, Vol. 76, No. 4, pp. 2005-2016, 2014.

[64] Z. Mazarei, M. Z. Nejad, A. Hadi, Thermo-elasto-plastic analysis of thick-walled spherical pressure vessels made of functionally graded materials, *International Journal of Applied Mechanics*, Vol. 8, No. 04, pp. 1650054, 2016.

[65] M. Shishesaz, A. Zakipour, A. Jafarzadeh, Magneto-Elastic Analysis of an Annular FGM Plate Based on Classical Plate Theory Using GDQ Method, *Latin American Journal of Solids and Structures*, Vol. 13, No. 14, pp. 2736-2762, 2016.

[66] M. Z. Nejad, N. Alamzadeh, A. Hadi, Thermoelastoplastic analysis of FGM rotating thick cylindrical pressure vessels in linear elastic-fully plastic condition, *Composites Part B: Engineering*, Vol. 154, pp. 410-422, 2018.

[67] M. Z. Nejad, A. Rastgoo, A. Hadi, Exact elasto-plastic analysis of rotating disks made of functionally graded materials, *International Journal of Engineering Science*, Vol. 85, pp. 47-57, 2014/12/01/, 2014.

[68] M. Bayat, M. Saleem, B. Sahari, A. M. S. Hamouda, E. Mahdi, Mechanical and thermal stresses in a functionally graded rotating disk with variable thickness due to radially symmetry loads, *International Journal of Pressure Vessels and Piping*, Vol. 86, No. 6, pp. 357-372, 2009.

[69] L. Chen, H. Chu, Hybrid laplace transform/finite element method for transient thermoelastic problem of composite hollow cylinder, *Computers & Structures*, Vol. 36, No. 5, pp. 853-860, 1990.

[70] P. Chen, Symmetric thermoelastic stress in cylinders by the lanczos-chebyshev method, *Nuclear Engineering and Design*, Vol. 55, No. 1, pp. 123-129, 1979.

[71] C. Jiunn-Ming, C. Cha'o-Kuang, C. Ming, Thermoelastic transient response of an infinitely long annular cylinder composed of three different materials, *Computers & structures*, Vol. 45, No. 2, pp. 229-236, 1992.

[72] Y. Yu-Ching, C. Cha'o-Kuang, Thermoelastic transient response of an infinitely long annular cylinder composed of two different materials, *International journal of engineering science*, Vol. 24, No. 4, pp. 569-581, 1986.

[73] H. Shodja, F. Ahmadpoor, A. Tehranchi, Calculation of the additional constants for fcc materials in second strain gradient elasticity: behavior of a nano-size Bernoulli-Euler beam with surface effects, *Journal of Applied Mechanics*, Vol. 79, No. 2, pp. 021008, 2012.

[74] *MatWeb*, Accessed; http://www.matweb.com.